EUROPEAN CENTRE FOR MEDIUM RANGE WEATHER FORECASTS

TECHNICAL REPORT NO. 8

****

NOVEMBER

1977

****

On the asymptotic behaviour of simple stochastic-dynamic systems

by

A. Wiin-Nielsen

European Centre for Medium Range Weather Forecasts

CONTENTS PAGE NUMBER

ABSTRACT

The investigation is concerned with the impact of initial uncertainties on predictions. The problem can be solved in an exact manner for sufficiently simple nonlinear systems where an exact solution of the deterministic non-linear problem is known. Examples of this kind are given in Sections 2, 3, 4 and 5 in which comparisons are made between exact and approximative solutions. The latter solutions are obtained either by simple closure schemes or by Monte Carlo calculations.

It is found from the examples that the behaviour at large times of a given system depends on the number of asymptotic steady states of the deterministic system and on the nature of the probability density function. Large deviations exist between the deterministic and approximative solutions if the initial uncertainties are non-negligible as compared to the mean values.

A closure scheme, based on the neglect of third and higher moments, may introduce steady states not present in the exact stochastic-dynamic treatment. The exact and approximative solutions are very different if the initial state is selected close to such a false steady state.

In some of the examples it is seen that the asymptotic values of the uncertainty may be less than the initial uncertainty. This behaviour may be due to the fact that the sum of the certain and uncertain energies is conserved.

1. Introduction

The problem of incorporating the initial uncertainties in an atmospheric prediction model has been considered by Epstein (1969), Fleming (1971a, b) and Pitcher (1974) who use a stochastic-dynamic approach. The statistical-dynamical methods in weather forecasting have been reviewed in detail by Leith (1975). The investigations quoted above concentrate in general on simple models of the atmosphere and apply furthermore to short-range predictions.

The incorporation of uncertainties in the initial state in predictions is not a problem unique to the atmospheric sciences, but applies to any scientific field in which predictions based on a quantitative model are made. Errors or uncertainties in the initial state will make the predictions uncertain. Even if the quantitative model were a true description of a natural phenomenon, we must expect that the predicted state is inaccurate because it is influenced by the uncertain initial state.

In a non-linear model we will often find that the uncertainty increases markedly during the first period of integration whereafter the uncertainty asymptotically approaches a level determined by the properties of the system. However, the behaviour of a given stochastic-dynamic system at large times has not been investigated in detail due to the extreme mathematical difficulties

in dealing with non linear systems. The present investigation is naturally also incapable of giving general results but it has been possible to treat some simple cases in detail. For these cases we can determine the asymptotic state either by analytical or numerical methods. Some of the examples are taken from the simple models which are used in determining the growth of populations in theoretical ecology while others are of a meteorological nature.

The fact that exact solutions of the stochastic-dynamic problems can be obtained in certain cases gives a possibility to compare these solutions with stochastic-dynamic solutions obtained from a certain closure assumption. Although the closure scheme in this paper is limited to the neglect of third and higher order moments, it is naturally possible to investiage other closure schemes by similar methods.

The behaviour of a stochastic-dynamic system at large times depends on whether or not asymptotic, steady states exist. In addition, it turns out that the properties of the probability density function are important for the asymptotic state of the dynamic system when it is considered from a stochastic point of view. If only one asymptotic steady state for the deterministic system exists within the region covered by the probability density function, it appears that the stochastic-dynamic prediction will also approach an asymptotic state which may or may not coincide with the deterministic steady

state. However, if the initial uncertainty is small, there is little difference in our examples between the deterministic and the stochastic-dynamic steady states. On the other hand, if two deterministic steady states exist within the region covered by the probability density function, it is found in our examples that the asymptotic steady state for the stochastic-dynamic system is between the deterministic steady states. Even more complicatedsituations are likely to appear if several deterministic steady states are present.

In some examples we find that the initial uncertainty gradually decreases and approaches zero at large time. In other examples it is found that the uncertainty, after an increase to a maximum, approaches a limiting value which in the cases considered here is smaller than the initial uncertainty. While it is impossible to make general conclusions from a few examples of an extremely simple nature, it is at least conceivable that such a behaviour may be characteristic for more realistic systems.

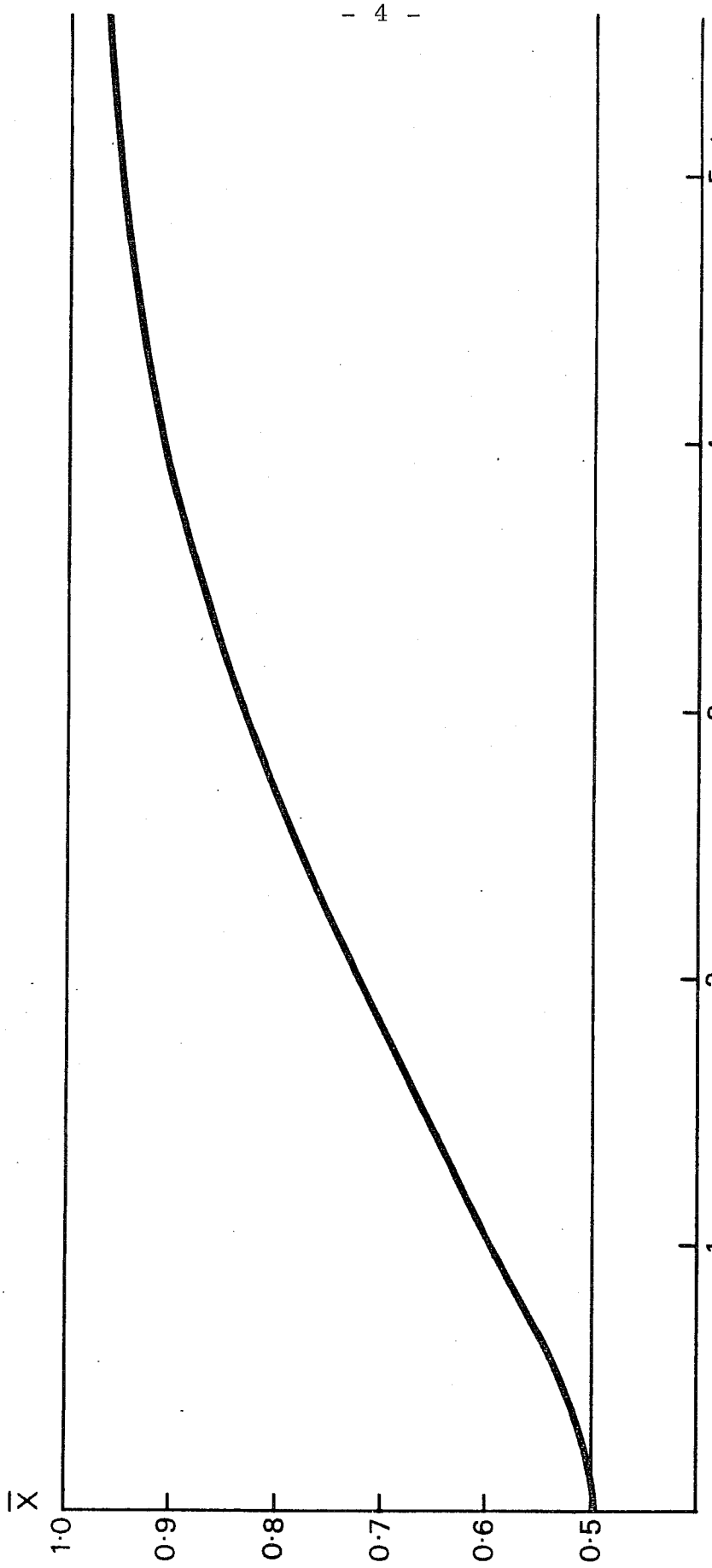

Fig. 1a : $\bar{x} = \bar{x}(t)$ with initial conditions $\bar{x}_o = 0.5$ and $\sigma_o = 0.5$ obtained from the closure solution (3.13) and (3.14).

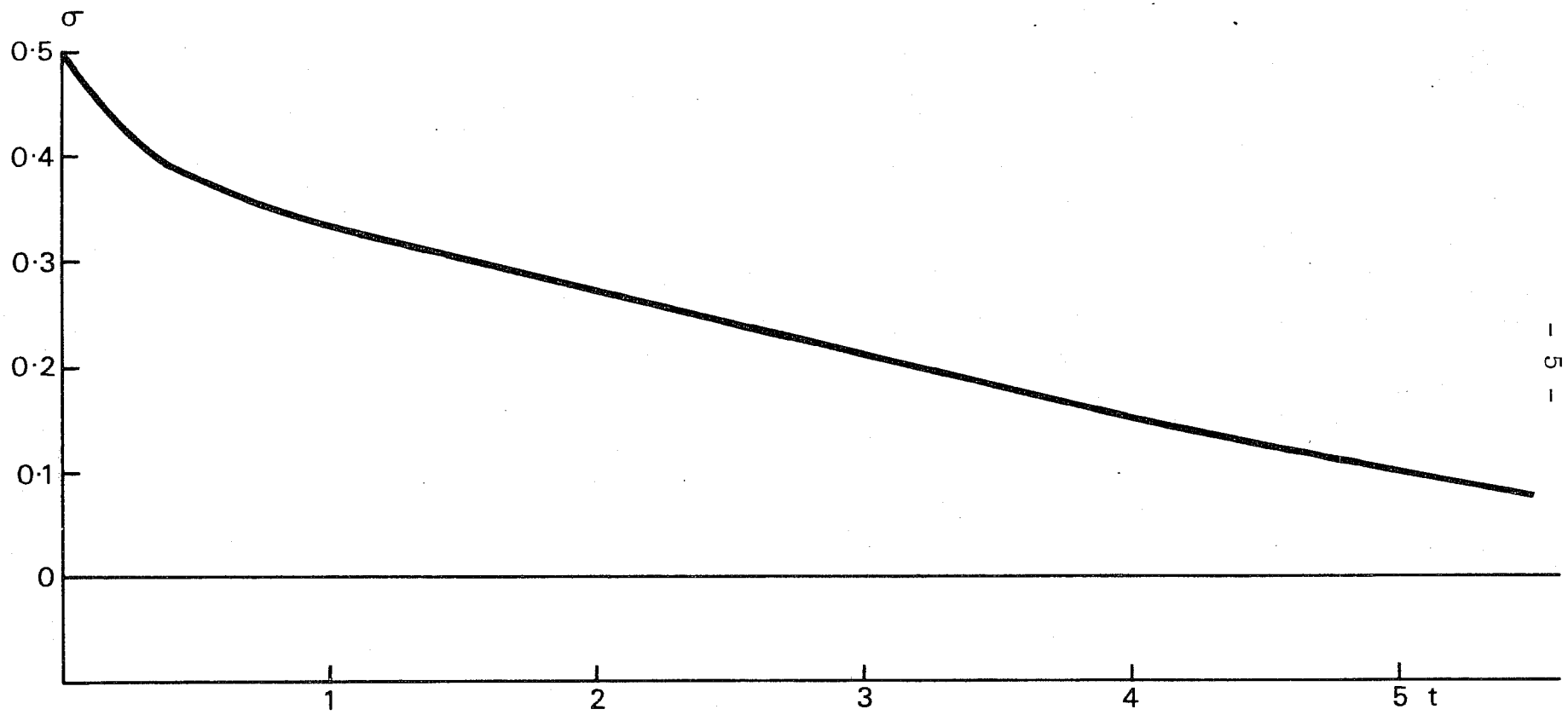

Fig. 1b : $\sigma = \sigma(t)$ with initial conditions $\bar{x}_0 = 0.5$ and $\sigma_0 = 0.5$ obtained from the closure solution (3.13) and (3.14).

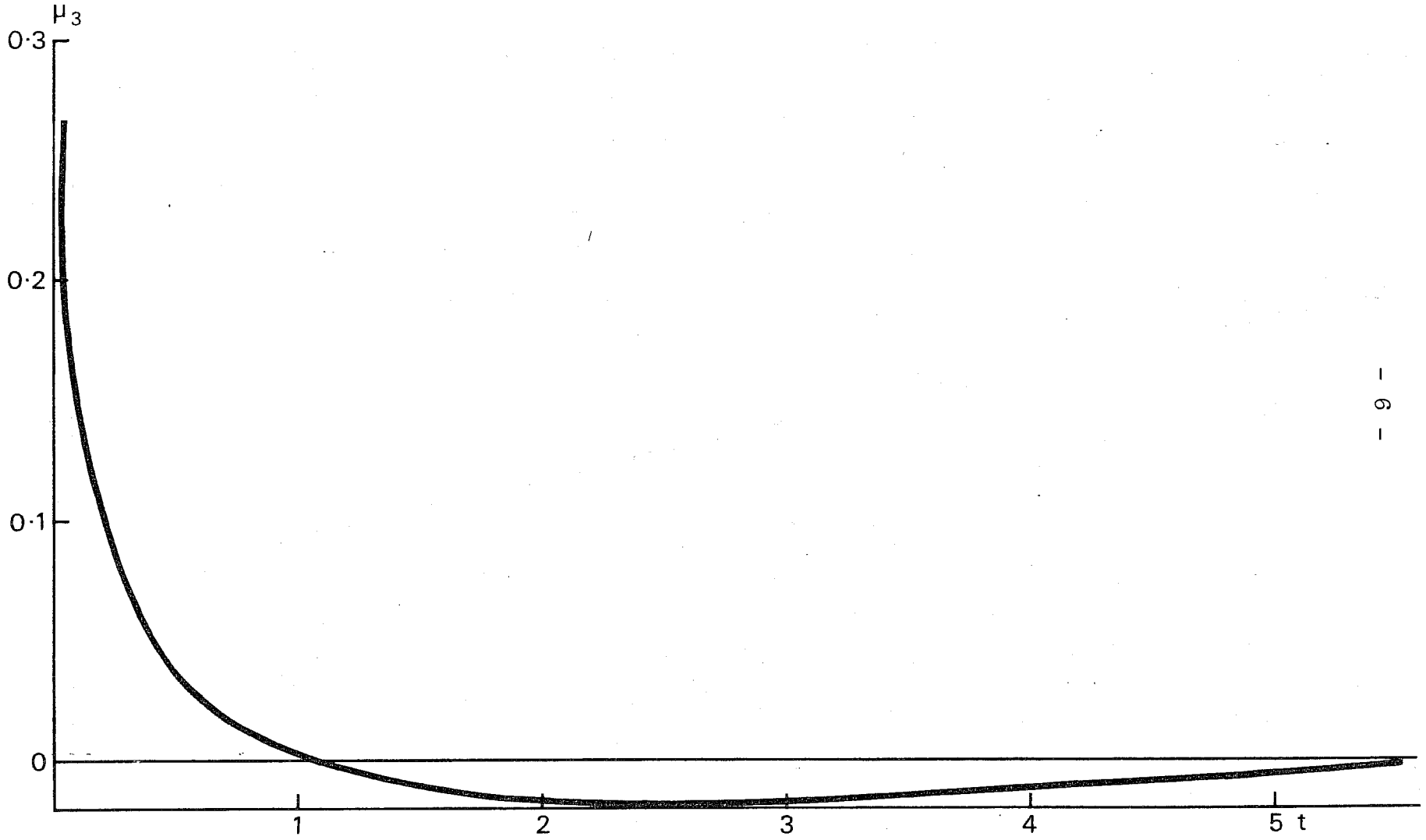

Fig. 1c : The third moment $\mu_3 = \mu_3(t)$ with the initial conditions $\bar{x}_o = 0.5$ and $\sigma_o = 0.5$ calculated from the closure solution (3.13) and (3.14).

2. A simple model for single populations

As our first example we shall select an equation much used in theoretical ecology (May, 1976) to illustrate a wide class of population equations with regulatory mechanisms of a nonlinear nature. For our purpose it is irrelevant that the equation cannot be taken seriously as a model of population growth because we shall use it to illustrate some aspects of a stochastic-dynamic treatment. In theoretical ecology the equation will usually have the form:

$$\frac{d\,N}{d\,\tau} = r\,N\,(1 - \frac{N}{K}) \quad , \tag{2.1}$$

in which N is the number of elements in the population, τ is the time, r is the "intrinsic" growth rate, and K is an equilibrium value of N. We note from (2.1) that if K is infinitely large, we have exponential growth determined by r. It is also seen that as long as $N < K$, N will be increasing, while $N = K$ represents a stationary point. For $N > K$, we find $d\,N\,/\,d\,\tau < 0$.

To get (2.1) in a more convenient form it is an advantage to nondimensionalise the variables. Defining

$$x = N\,/\,K, \quad t = r\,\tau \quad , \tag{2.2}$$

we find that (2.1) takes the form

$$\frac{d\,x}{d\,t} = x\,(1 - x)\ . \qquad (2.3)$$

The solution of (2.3) is

$$x = \frac{x_o}{x_o - (x_o - 1)\,e^{-t}}\ , \qquad (2.4)$$

for the initial condition $x = x_o$, $t = 0$. $x > 0$ in a study of population growth. In this case we find from (2.4) if $x_o > 0$, we will have $x > 0$ for all t.

We shall now turn our attention to a stochastic-dynamic treatment of (2.3). The idea is that the initial state is not known with absolute certainty. It will be assumed that the initial state is given by a probability density function $\phi\,(x, t_o)$. As shown by Pitcher (1974) and others $\phi(x, t)$ satisfies a continuity equation expressing the conservation law for probability. However, even more important for this example Pitcher (loc. cit.) shows that the expected value of x can be calculated from the formula

$$\bar{x} = E\,(x) = \int_{-\infty}^{+\infty} x\,(x_o,\ t)\ \phi_o\,(x_o, t_o)\ dx_o\ . \qquad (2.5)$$

The significance of (2.5) is that the integration is carried out over x_o using the values of $\phi\,(x, t)$ for $x = x_o$ and $t = 0$, i.e. (2.5) may be calculated without even computing ϕ for $t > 0$. However, $\bar{x} = \bar{x}\,(t)$ may be calculated for $t > 0$ because of the time dependence in $x\,(x_o, t)$. We shall make use of (2.5) to calculate $\bar{x} = \bar{x}\,(t)$ in our example. To do this, we must assume some

form of $\phi_o\ (x_o, t_o)$.

In our specific case we are considering a problem in which $x \geq 0$. It is thus natural to select a probability density function which is positive for $x > 0$ but by definition equal to zero for $x < 0$. One probability density function satisfying these criteria is the Pearson type III function defined by

$$\phi\ (x) = \begin{cases} \dfrac{1}{\beta^p\ \Gamma(p)} \cdot x^{p-1}\ e^{-\frac{x}{\beta}}, & x \geq 0 \\ 0, & x < 0 \end{cases} \qquad (2.6)$$

in which β and p are constants. It is easy to calculate the mean and variance from the definition (2.6). The mean is $\bar{x} = \beta\ p$ while the variance is $\sigma^2 = p\ \beta^2$. It is thus seen from these expressions that given the mean value $\bar{x}$ and the variance σ^2 we may calculate the parameters

$$p = \frac{\bar{x}^2}{\sigma^2}, \quad \beta = \frac{\sigma^2}{\bar{x}} \quad . \qquad (2.7)$$

Using (2.6) and (2.4) in (2.5) we find that

$$\bar{x} = \bar{x}\ (t) = \int_o^\infty \frac{x_o}{\alpha\ x_o + 1 - \alpha_o} \frac{1}{\beta^p\ \Gamma(p)} x_o^{p-1}\ e^{-\frac{x_o}{\beta}}\ dx_o \qquad (2.8)$$

where

$$\alpha = 1 - e^{-t} \quad . \tag{2.9}$$

(2.8) may be evaluated by introducing the new variables

$$x = \beta \, a \, z \, , \qquad a = \frac{1}{\beta} \, \frac{1 - \alpha}{\alpha} \quad . \tag{2.10}$$

We find from (2.8) that

$$\bar{x} = \frac{\alpha^p}{\alpha \Gamma(p)} \int_0^\infty \frac{z^p}{1 + z} \, e^{- az} \, dz \quad . \tag{2.11}$$

According to Gradshteyn and Ryzhik (1965), we have

$$\int_0^\infty \frac{z^p}{1 + z} \, e^{- az} \, dz = e^{a} \, \Gamma(p + 1) \, \Gamma(-p, a), \tag{2.12}$$

where $\Gamma(-p, a)$ is the incomplete Gamma function. However, from Abramowitz and Stegun (1965), we have

$$E_{p+1}(a) = a^p \, \Gamma(-p, a) \, . \tag{2.13}$$

where $E_{p+1}(a)$ is the exponential integral (for details see Appendix 4).

It follows therefore that

$$\int_0^\infty \frac{z^p}{1+z}\, e^{-az}\, dz = \frac{e^a\, \Gamma(p+1)}{a^p}\, E_{p+1}(a) \qquad (2.14)$$

and, finally, that

$$\bar{x}(t) = \frac{e^a}{\alpha}\, p\, E_{p+1}(a)\,. \qquad (2.15)$$

We note from (2.10) that

$$\alpha^{-1} = 1 + \beta a \qquad (2.16)$$

and

$$t = \ln.\ (1 + \frac{1}{\beta a})\,. \qquad (2.17)$$

The formulas (2.15) - (2.17) are sufficient to calculate $\bar{x} = \bar{x}(t)$ noting that $E_n(a)$ are tabulated functions for the values n = 1, 2, 3, 4, 10 and 20. Values for other parameters may be obtained by the recurrence relation

$$E_{n+1}(a) = \frac{1}{n}\left[e^{-a} - a\, E_n(a) \right] \qquad (2.18)$$

The second moment may be calculated if we know the integral

$$m_2(t) = \int_0^\infty \frac{x_o^2}{(\alpha x_o + 1-\alpha)^2} \frac{1}{\beta^p \Gamma(p)} x_o^{p-1} e^{\frac{-x_o}{\beta}} dx_o \quad . (2.19)$$

Using the transformation (2.10) we get

$$m_2(t) = \frac{a^p}{\alpha^2 \Gamma(p)} \int_0^\infty \frac{z^{p+1}}{(1+z)^2} e^{-az} dz \quad . \qquad (2.20)$$

The most convenient way to obtain the integral (2.20) is to note that by setting az = y in (2.14), we may obtain:

$$\int_0^\infty \frac{y^p}{y+a} e^{-y} dy = e^a \Gamma(p+1) E_{p+1}(a) . \qquad (2.21)$$

The same substitution in (2.20) leads to

$$m_2(t) = \frac{1}{\alpha^2 \Gamma(p)} \int_0^\infty \frac{y^{p+1}}{(y+a)^2} e^{-y} dy, \qquad (2.22)$$

which may be written in the form

$$m_2(t) = -\frac{1}{\alpha^2 \Gamma(p)} \frac{d}{da} \left[\int_0^\infty \frac{y^{p+1}}{(y+a)} e^{-y} dy \right] . \qquad (2.23)$$

Upon evaluation, we get

$$m_2(t) = \frac{1}{\alpha^2} p(p+1) e^a \left[E_{p+1}(a) - E_{p+2}(a) \right] \qquad (2.24)$$

and we may now obtain:

$$\sigma(t)^2 = m_2(t) - \bar{x}(t)^2 \tag{2.25}$$

As we shall see later, it is normally not possible to obtain the exact integrals (2.15) and (2.24) in applications because they cannot be expressed in known tabulated functions. In these cases, it is therefore necessary to solve the problems by a closure approximation. A simple, but frequently used closure assumption is the neglect of third and higher moments. In our own simple case it is possible to test such a closure assumption because we can evaluate the third moment exactly. We begin by calculating

$$m_3(t) = \int_0^{\infty} \frac{x_o^3}{(\alpha x_o + 1 - \alpha)^3} \frac{1}{\beta^p \Gamma(p)} x_o^{p-1} e^{-\frac{x_o}{\beta}} dx_o . \tag{2.26}$$

The same transformations as before yield

$$m_3(t) = \frac{1}{\alpha^3 \Gamma(p)} \int_0^{\infty} \frac{y^{p+2}}{(y+a)^3} e^{-y} dy, \tag{2.27}$$

which may be treated as follows

$$m_3(t) = -\frac{1}{2} \frac{1}{\alpha^3 \Gamma(p)} \frac{d}{da} \left[\int_0^{\infty} \frac{y^{p+2}}{(y+a)^2} e^{-y} dy \right] . \tag{2.28}$$

We find therefore upon evaluation

$$m_3(t) = \frac{1}{2} \frac{p(p+1)(p+2)}{\alpha^3} e^a \left[E_{p+1}(a) - 2E_{p+2}(a) + E_{p+3}(a) \right] . \tag{2.29}$$

(2.29) may be used to calculate $m_3(t)$, and the third moment may then be calculated from the formula

$$\mu_3(t) = m_3(t) - 3\bar{x}(t)m_2(t) + 2\bar{x}^3 . \tag{2.30}$$

We note first of all that the initial value of μ_3 is different from zero in our example due to the fact that we are using a Pearson type distribution. This may be verified in our case by evaluating (2.29) for $t \to 0$, i.e. $a \to \infty$. Using the asymptotic expansion of $E_p(a)$ for all three terms in (2.29) we find that

$$\lim_{t \to 0} m_3(t) = \beta^3 p(p+1)(p+2) .$$

Using (2.30) we find then that

$$\mu_3(0) = 2p\beta^3 = 2 \frac{\sigma_o^4}{\bar{x}_o} \tag{2.31}$$

$\mu_3(0)$ is thus small whenever $\sigma_o << (\bar{x}_o)^{\frac{1}{4}}$.

On the other hand, for large values of t we find that

$$\lim_{t\to\infty} m_3(t) = 1 \ , \tag{2.32}$$

and according to (2.30)

$$\lim_{t\to\infty} \mu_3(t) = 0 \ . \tag{2.33}$$

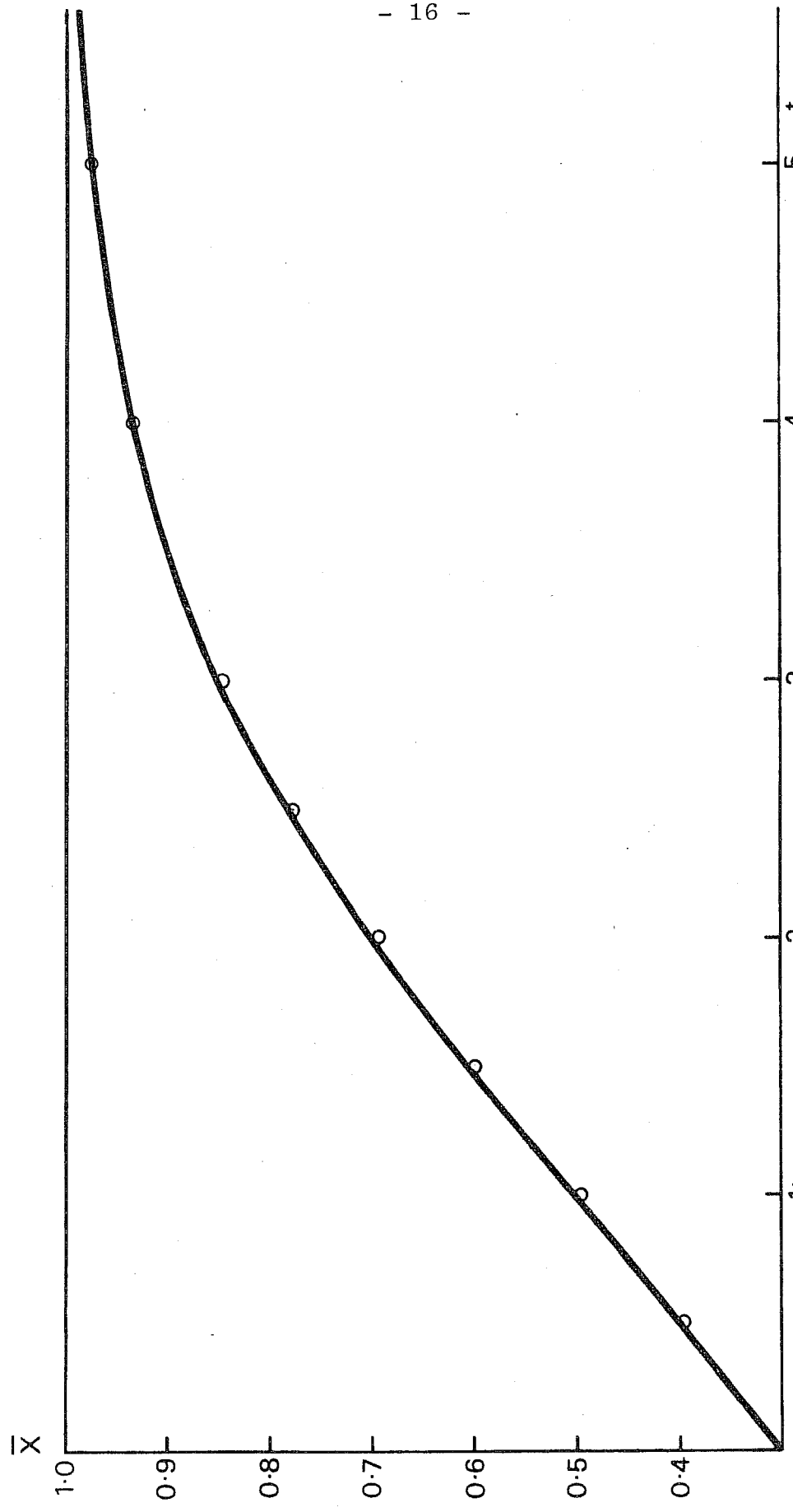

Fig. 2a : $\bar{x} = \bar{x}(t)$ with initial conditions $\bar{x}_o = 0.3$ and $\sigma_o = 0.1732$, corresponding to $p = 3$ and $\beta = 0.1$, calculated from (2.15). The small circles are points $\underline{x} = \bar{x}(t)$ calculated from the closure solution (3.13) and (3.14).

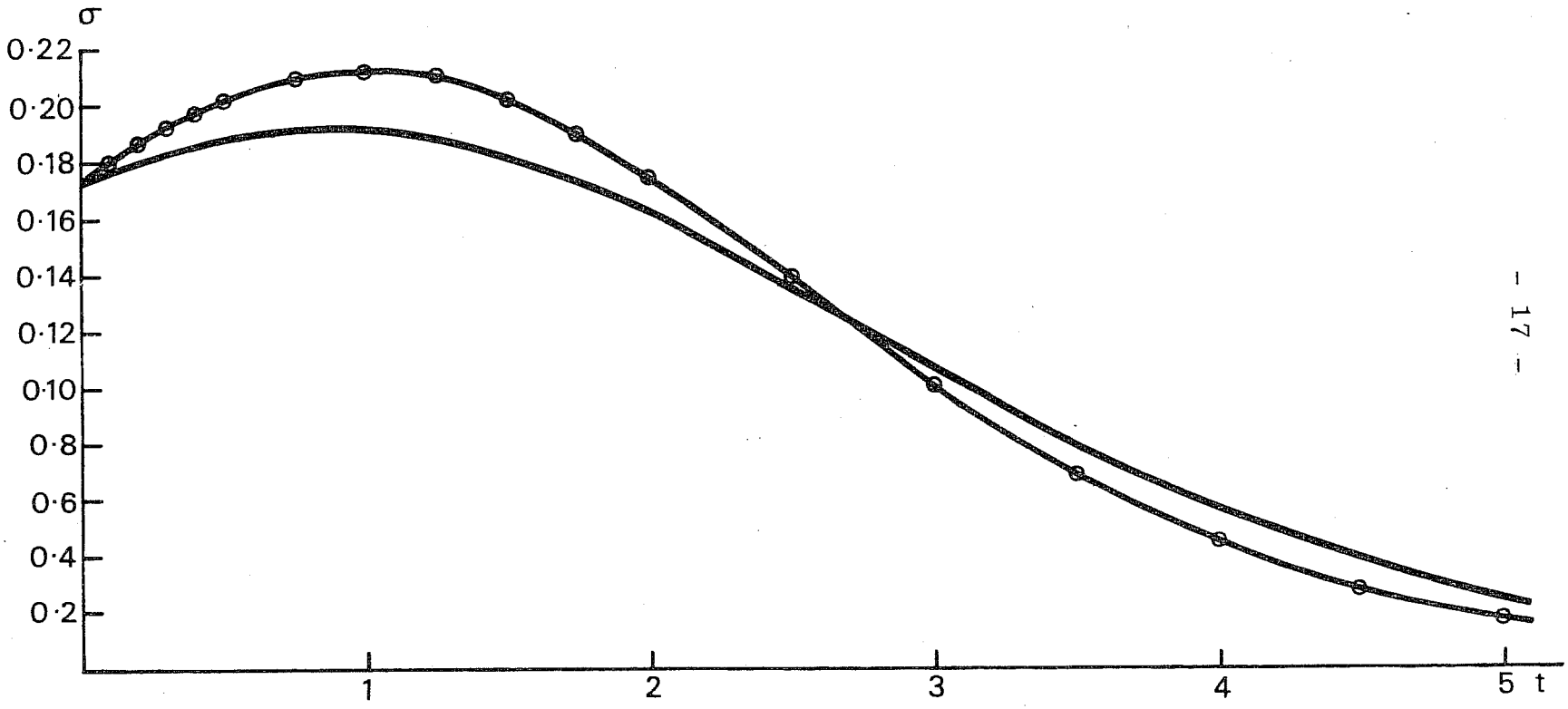

Fig. 2b : $\sigma = \sigma(t)$ with initial conditions $\bar{x}_o = 0.3$ and $\sigma_o = 0.1732$, calculated from (2.24) and (2.25). The curve with the small circles is $\sigma = \sigma(t)$ with the same initial conditions computed from (3.13) and (3.14).

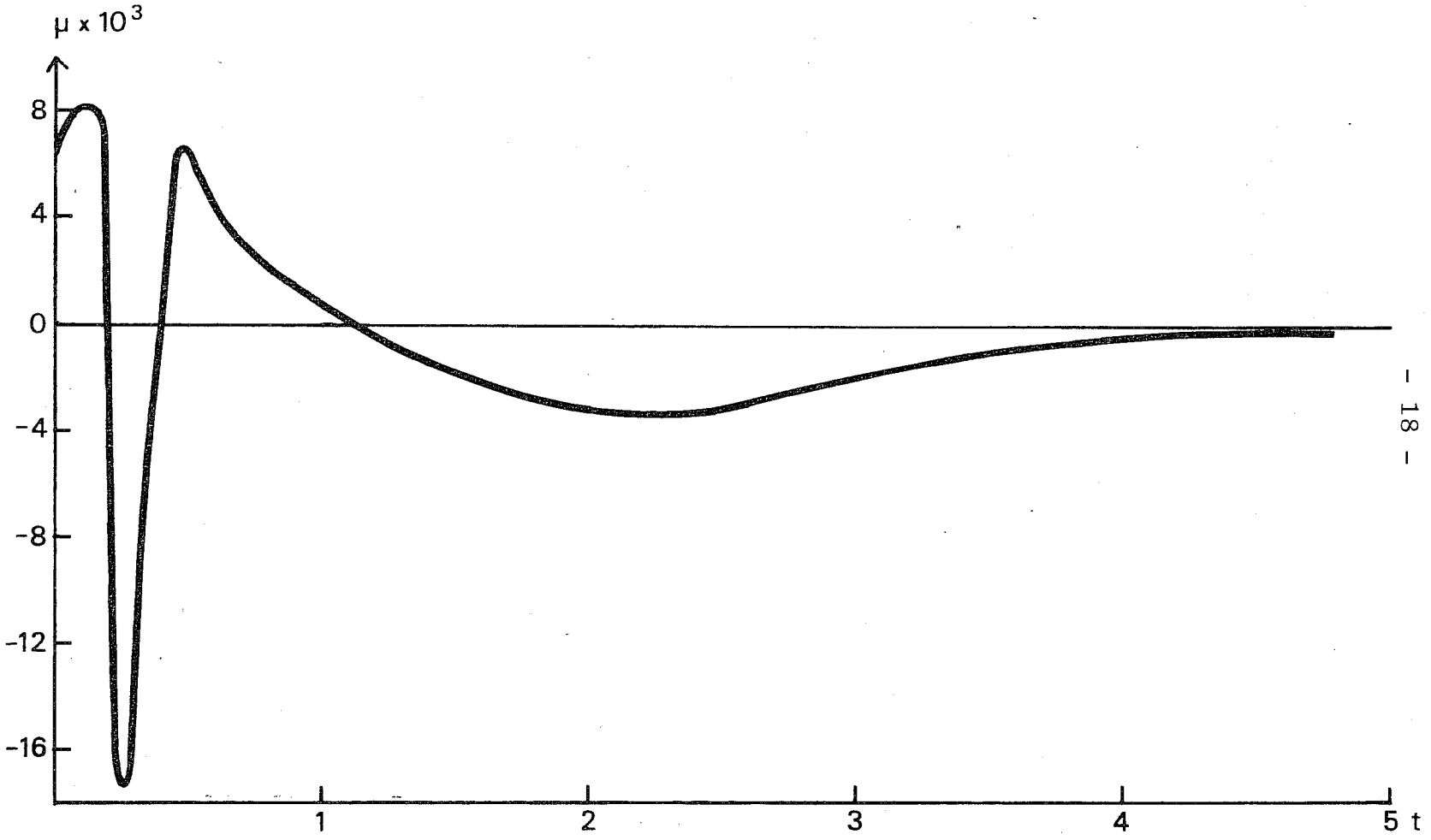

Fig. 2c : The third moment $\mu_3 = \mu_3(t)$ with the initial conditions $\bar{x}_o = 0.3$ and $\sigma_o = 0.1731$ calculated from (2.29) and (2.30).

3. Solution by a closure assumption

It is normally not possible to provide an analytical treatment as given in the previous section because the integrals cannot be expressed in known tabulated functions or because the deterministic equation cannot be solved in a closed form. The common procedure in these cases is to replace the deterministic equation by an infinite set of equations which express the rate of change of the various moments of the probability distribution. The set becomes infinite because the equation for a given moment requires information of a higher moment. In practical applications it is thus necessary to introduce a closure assumption which results in a finite set. Most common among the closure assumptions is the neglect of the third and higher moments. We shall use this closure approximation to provide a second solution to the equation considered in Section 2. It will thus be possible to compare the exact solutions provided earlier to the new approximate solution. Our starting point is equation (2.3). We introduce the notations:

$$
\begin{aligned}
\bar{x} &= E(x) \\
\mu_2 &= E\left[(x-\bar{x})^2\right] = E(x^2) - \bar{x}^2 = \sigma^2 \\
\mu_3 &= E\left[(x-\bar{x})^3\right] = E(x^3) - 3\bar{x}\mu_2 - \bar{x}^3 \\
\mu_4 &= E\left[(x-\bar{x})^4\right] = E(x^4) - 4\bar{x}\mu_3 - 6\bar{x}^2\mu_2 - \bar{x}^4
\end{aligned}
\qquad (3.1)
$$

Applying the operator E to (2.3) we find

$$\frac{d\bar{x}}{dt} = \bar{x} - \bar{x}^2 - \mu \qquad (3.2)$$

where we have written $\mu = \mu_2$.

An equation for $d\mu / dt$ can be obtained from the second expression in (3.1) by differentiation with respect to time, i.e.

$$\frac{d\mu}{dt} = E\left(2x \frac{dx}{dt}\right) - 2\bar{x} \frac{d\bar{x}}{dt} \quad . \qquad (3.3)$$

Evaluation of the expression in (3.3) leads to

$$\frac{d\mu}{dt} = 2\mu\ (1 - 2\bar{x}) \qquad (3.4)$$

where we have neglected the contribution from the third moment. The remaining part of this section is devoted to obtaining a solution in closed form of the system (3.2) and (3.4). We note that in most applications it is impossible to obtain such a solution and the equations must then be solved by numerical methods, but in our simple example we can reduce the system (3.2) and (3.4) to a solvable nonlinear differential equation. We introduce the new variable

$$y = \ln.\mu, \quad \mu = e^y \qquad (3.5)$$

The system becomes

$$\frac{d\bar{x}}{dt} = \bar{x} - \bar{x}^2 - e^y$$
$$\bar{x} = \frac{1}{2} - \frac{1}{4}\frac{dy}{dt} \quad . \tag{3.6}$$

Substituting from the second into the first equation of (3.6) we get

$$\frac{d^2y}{dt^2} - \frac{1}{4}\left(\frac{dy}{dt}\right)^2 = 4\ e^y - 1 \ . \tag{3.7}$$

(3.7) can be reduced to a first order equation by writing

$$p = p(y) = \left(\frac{dy}{dt}\right)^2 \tag{3.8}$$

and we find:

$$\frac{dp}{dy} - \frac{1}{2}p = 8\ e^y - 2 \tag{3.9}$$

with the solution

$$p = (16\ e^y + 4) + C_o\ e^{\frac{1}{2}y} = 16\ \mu + 4 + C_o\ \sqrt{\mu} \ . \tag{3.10}$$

The integration constant C_o is determined by the initial conditions, $\bar{x} = \bar{x}_o$, $\mu = \mu_o$ at $t = 0$

We find that

$$C_o = \frac{16}{\sqrt{\mu_o}} \left[\bar{x}_o(\bar{x}_o-1) - \mu_o \right] . \qquad (3.11)$$

Introducing finally $\sigma = \sqrt{\mu}$, we may write (3.10) in the form

$$\left(\frac{d\sigma}{dt}\right)^2 = \sigma^2 \ (4\sigma^2 + \tfrac{1}{4}C_o\sigma + 1) \quad . \qquad (3.12)$$

(3.12) can be solved in a straightforward way by separation of variables. We obtain first t as a function of σ and Co. However, this expression may after some manipulation be written in the form

$$\sigma = \sigma_o \frac{e^{-t}}{\left[(\bar{x}_o-\sigma_o)-(\bar{x}_o-\sigma_o-1)e^{-t} \right]\left[(\bar{x}_o+\sigma_o)-(\bar{x}_o+\sigma_o-1)e^{-t} \right]} , \qquad (3.13)$$

while $\bar{x} = \bar{x}(t)$ may be obtained using the second equation in (3.6) giving

$$\bar{x} = \tfrac{1}{2}\left[1 \pm (1+\tfrac{1}{4}C_o\sigma+4\sigma^2)^{\frac{1}{2}} \right] \qquad (3.14)$$

with

$$\tfrac{1}{4}C_o = \frac{4}{\sigma_o}\left[\bar{x}_o(\bar{x}_o-1) - \sigma_o^{\,2} \right] \qquad (3.15)$$

The double sign in (3.14) is to be understood in such a way that we select the sign giving $\bar{x} = \bar{x}_0$ when $\sigma = \sigma_0$. (3.13) - (3.15) provide thus the detailed solution in a closed form.

The solution obtained from the closure approximation has some properties which are different from the exact solution given in Section 2. For example, if $\bar{x}_0 = \sigma_0 = 0.5$, we find from (3.13) that $\bar{x} = \sigma = 0.5$ at all times. This behaviour is not found in the exact solution. Furthermore, in the case of $\bar{x}_0 = \sigma_0$, it is seen that $\sigma = \sigma(t)$ is

$$\sigma = \frac{\sigma_0}{2\sigma_0 - (2\sigma_0 - 1)e^{-t}} \qquad (3.16)$$

and it follows from this formula that $\lim_{t\to\infty} \sigma = 0.5$ and therefore that $\lim_{t\to\infty} \bar{x} = 0.5$. Apart from these special cases, we find that $\lim_{t\to\infty} \sigma = 0$ and $\lim_{t\to\infty} \bar{x} = 1$, in agreement with the exact solution.

The case $\bar{x}_0 = \sigma_0 = 0.5$ is illustrated in Figure 1a, b, and c. Figures 1a and 1b show that the closure solution ($\bar{x} = \sigma = 0.5$) deviates radically from the exact solution. Figure 1c shows that the third moment μ_3 becomes small and negative rather rapidly before it goes to zero for large times. The case illustrated in Figure 1 is very special because it is a steady state in the equations after the closure assumption has been introduced. A more typical case is shown in Figure 2a, b and c. The parameters are

$\bar{x}_0 = 0.3$, $\sigma_0 = 0.1732 = 0.03^{\frac{1}{2}}$ corresponding to $p = 3$, $\beta = 0.1$. Figure 2a shows the exact solution $\bar{x} = \bar{x}(t)$. Points from the closure solution have been given by small circles. It is seen that a good agreement exists between the two solutions for $\bar{x}$. Larger differences exist between the exact and closure solutions for $\sigma = \sigma(t)$ as shown in Fig. 2b. The third moment calculated from the exact solution is shown in Fig. 2c. After some oscillations for small t, μ_3 approaches zero.

Figure 3a, b and c illustrate a case where $\bar{x}_0 = 19^{\frac{1}{2}} = 4.36$, $\sigma_0 = 1$ corresponding to $p = 19$, $\beta = 19^{-\frac{1}{2}} = 0.23$. Fig. 3a and 3b show a very good agreement between the exact and closure solutions for both $\bar{x}$ and σ. This is due to the fact that the third moment shown in Fig. 3c is small initially and remains so for all times.

The model used in Sections 2 and 3 has been limited to positive values of x because it applies to a given population. However, as a mathematical model it has nevertheless solutions if $x_0 < 0$, but these solutions will approach $-\infty$ for a finite value of time. Due to the fact that we have selected the probability density function (2.6) which is limited to the positive domain, we have not had to consider the solutions for $x_0 < 0$. It is of interest to consider the stochastic-dynamic solution briefly in such a case. We may easily do this by assuming that the function (2.6) is replaced by a Gaussian distribution, i.e.

$$\phi(x) = \frac{1}{\sigma\sqrt{2\pi}} \exp\left[-\left(\frac{x-\bar{x}}{\sigma\sqrt{2}}\right)^2 \right] \tag{3.17}$$

in which case $\bar{x} = \bar{x}(t)$ is calculated from the following integral

$$\bar{x} = \int_{-\infty}^{+\infty} \frac{x_o}{\alpha x_o + 1 - \alpha} \frac{1}{\sigma_o\sqrt{2\pi}} e^{-\left[\frac{x_o - \bar{x}_o}{\sigma_o\sqrt{2}}\right]^2} dx_o \ . \tag{3.18}$$

Since the integration with respect to x_o covers the whole region from $-\infty$ to $+\infty$, it is obvious that the intergrand for each value of $\alpha = \alpha(t)$ will go to infinity. We cannot be sure that the integral (3.18) is finite under these conditions. It turns out in this particular case that $\bar{x} = \bar{x}(t)$ is finite for all t as we shall show below.

We introduce the transformation

$$\xi = \frac{x_o - \bar{x}_o}{\sigma_o\sqrt{2}} \tag{3.19}$$

and obtain

$$\bar{x} = \frac{1}{\alpha} - \frac{1-\alpha}{\alpha^2\sigma_o\sqrt{2}} \frac{1}{\sqrt{\pi}} \int_{-\infty}^{+\infty} \frac{1}{\xi + n} e^{-\xi^2} d\xi \tag{3.20}$$

where

$$n = \frac{\alpha\bar{x}_o + 1 - \alpha}{\alpha\sigma_o\sqrt{2}} \ .$$

Introducing further

$$z = \xi + n \tag{3.22}$$

we find that

$$\bar{x} = \frac{1}{\alpha}\left[1 - \frac{(1-\alpha)}{\alpha\sigma_o\sqrt{2}}\ \frac{1}{\sqrt{\pi}}\int_{-\infty}^{n}\frac{1}{z}\ e^{-(z-n)^2}\ dz\right] \tag{3.23}$$

The integral in (3.23) has been evaluated in Appendix 1 of this paper. Using the result from (A12) we may finally write

$$\bar{x} = \frac{1}{\alpha}\left[1 + \frac{1-\alpha}{\alpha}\ \frac{\sqrt{2}}{\sigma_o}\ D(n)\right] \tag{3.24}$$

where D(n), known as Dawson's integral, is

$$D(n) = e^{-n^2}\int_{o}^{n} e^{s^2}\ ds\ . \tag{3.25}$$

D(n) is a tabulated integral. We note from (3.24) that for $t \to \infty$, $\alpha \to 1$ we find $\bar{x} \to 1$. In spite of the fact that x(t) is unlimited for negative values of x we find therefore that $\bar{x}(t)$ is finite and well behaved. Figure 4 shows an example calculated for $\bar{x}_c = 1.1$, $\sigma_o = 0.5$ using (3.21) and (3.24) for the calculations. It should also be pointed out that the integral $m_2(t)$ using the Gaussian distribution is infinite, and it is thus not possible to complete the whole analysis in this case.

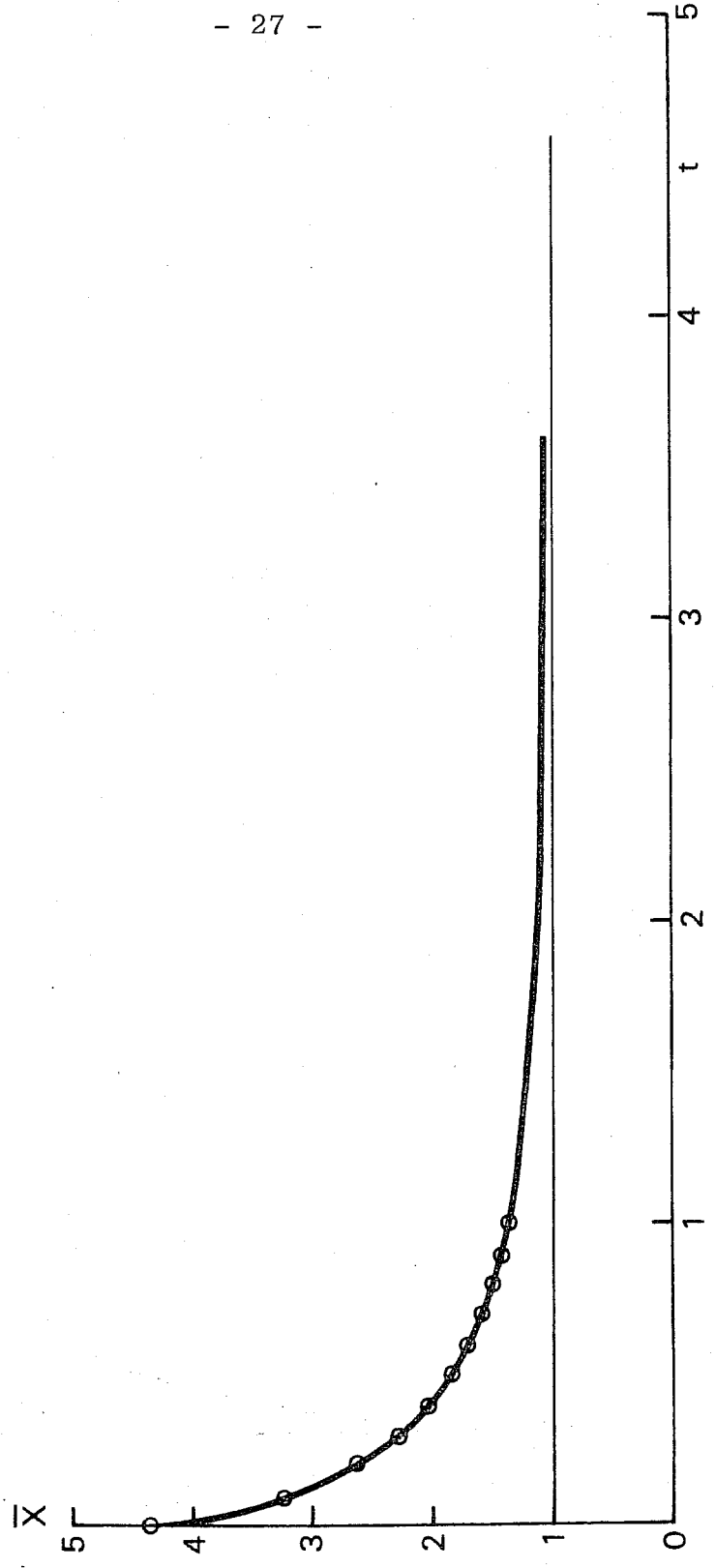

Fig. 3a : Initial conditions are $\bar{x}_o = 19^{\frac{1}{2}}$, $\sigma_o = 1$, corresponding to p = 19, $\beta = 19^{-\frac{1}{2}}$. Arrangement as in Fig. 2a.

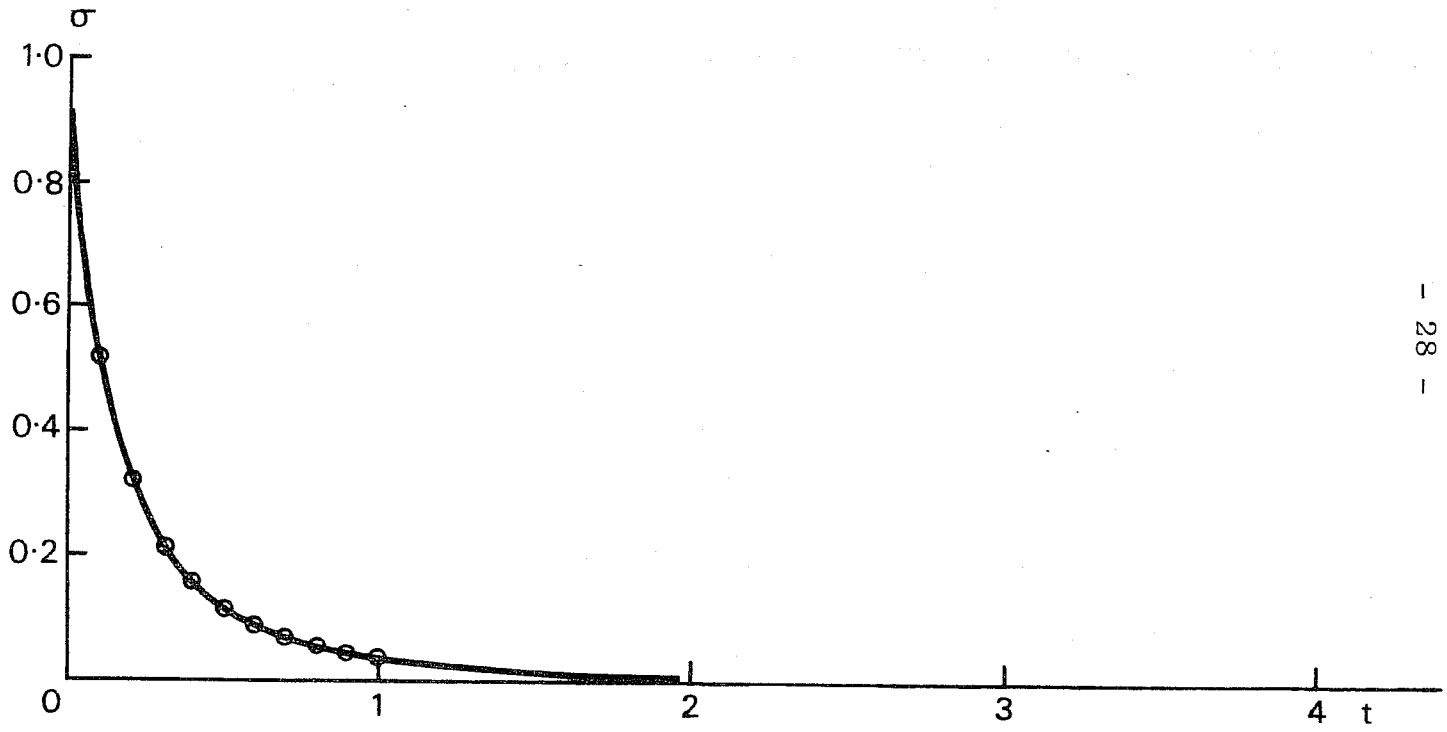

Fig. 3b : Initial conditions $\bar{x}_0 = 19^{\frac{1}{2}}$, $\sigma_0 = 1$, corresponding to $p = 19$, $\beta = 19^{-\frac{1}{2}}$. Arrangement as in Fig. 2b.

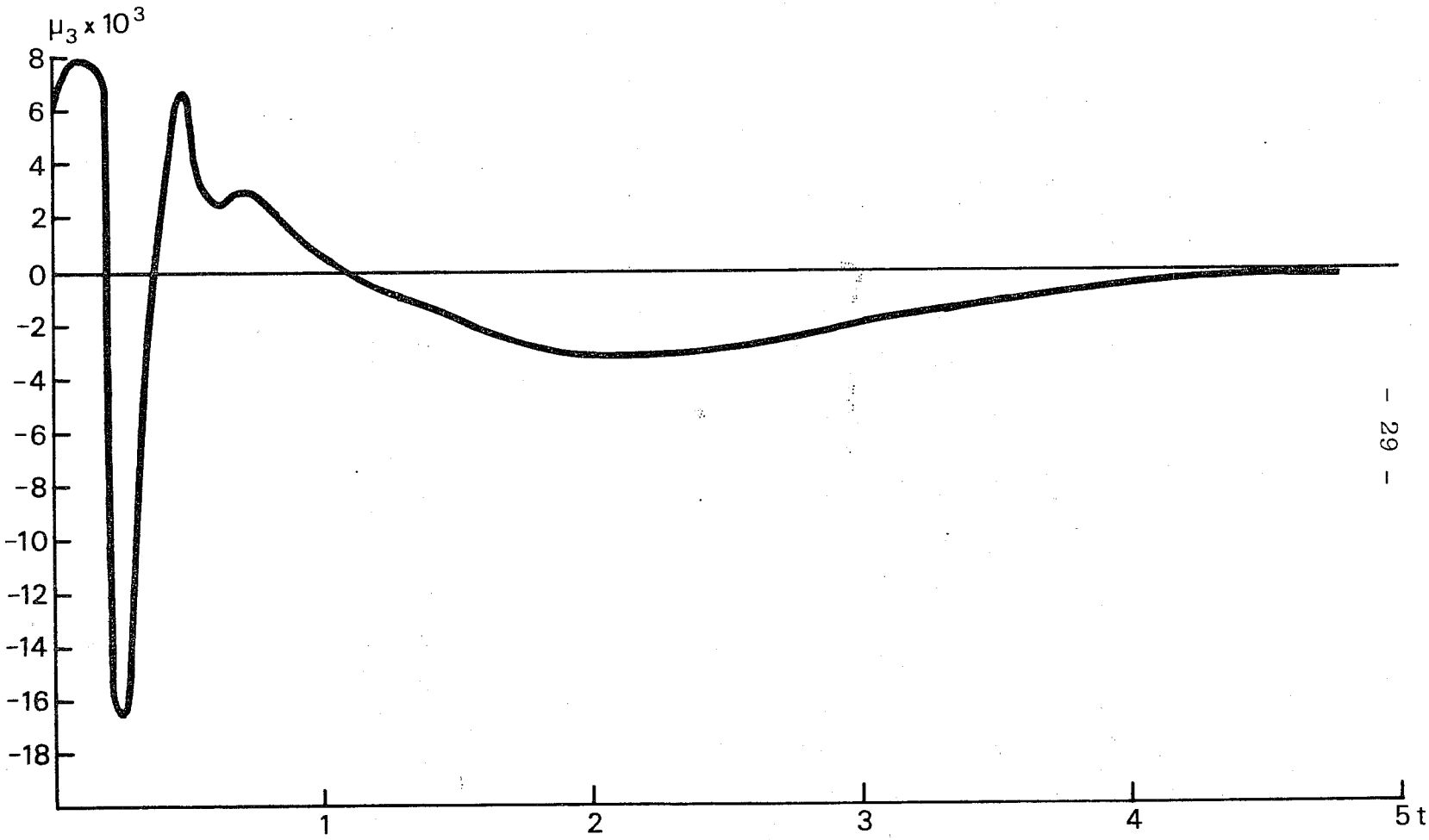

Fig. 3c : Initial conditions $\tilde{x}_0 = 19^{\frac{1}{2}}$, $\sigma_0 = 1$, corresponding to $p = 19$, $\beta = 19^{-\frac{1}{2}}$. Arrangement as in Fig. 2c.

4. Another simple model

The example treated in Sections 2 and 3 is the most simple model for the changes in a population of a single species. More complicated models exist, but we shall select a second example which to a large extent can be solved in terms of known functions using the stochastic dynamic approach. We shall furthermore select our example in such a way that $x = x(t)$ is finite for all x at all times. It is assumed that the population is governed by the equation

$$\frac{dx}{dt} = x - x^3 . \tag{4.1}$$

The deterministic solution is most easily obtained by introducing $y = x^2$ leading to

$$\frac{dy}{dt} = 2y - 2y^2 , \tag{4.2}$$

with the solution

$$y = \frac{y_o}{y_o - (y_o - 1)e^{-2t}} , \tag{4.3}$$

where $y_o = x_o^2$ and x_o is the value of x for $t = 0$. We get therefore

$$x = \frac{x_o}{(\alpha x_o^2 + 1 - \alpha)^{\frac{1}{2}}} \tag{4.4}$$

where α in this case is defined by

$$\alpha = 1 - e^{-2t} \quad . \tag{4.5}$$

We note from (4.1) that three stationary states exist, i.e. $x = 0$, $x = -1$ and $x = 1$. It is apparent that of these $x = 0$ is an unstable stationary state while $x = -1$ and $x = 1$ are stable. In addition, for $x_o > 0$, we find $x > 0$ for all t and $\lim_{t\to\infty} x = 1$, while $x_o < 0$ leads to $x < 0$ for all t with $\lim_{t\to\infty} x = -1$.

We shall again seek to make a stochastic dynamic treatment, i.e. we want to evaluate

$$\bar{x} = \bar{x}(t) = \int_{-\infty}^{+\infty} x(x_o, t)\ \phi\ (x_o,\ t_o)\ dx_o \quad . \tag{4.6}$$

The present example is more interesting than the previous one because we have two possible asymptotic deterministic states, $x = 1$, and $x = -1$. If we want to avoid any difficulties from, say, $x = -1$, we may naturally do so by selecting a probability density function $\phi(x)$ having non-zero values only for $x > 0$. A suitable candidate is then the function $\phi(x)$ defined by (2.6), and this is the choice which should be made if x represents the number of elements in a population. On the other hand, if the

physical nature of x is such that it can take both positive and negative values, we would rather select a distribution of the type (3.17), i.e. a normal distribution. Since we do not have a particular interpretation in mind, we shall investigate both cases.

Starting with the the Gaussian distribution, we must consider the integral

$$\bar{x} = \frac{1}{\sigma_o \sqrt{2\pi}} \int_{-\infty}^{+\infty} \frac{x_o}{(\alpha x_o^2 + (1-\alpha))^{\frac{1}{2}}} e^{-\left(\frac{x_o - \bar{x}_o}{\sigma_o \sqrt{2}}\right)^2} dx_o . \quad (4.7)$$

Before we consider the evaluation for an arbitrary value of t we shall consider the value of (4.7) as $t \to \infty$. We note then that for $t \to \infty$ we have $\alpha = 1$ giving $x(x_o, \infty) = 1$ for $x_o > 0$ and $x(x_o, \infty) = -1$ for $x_o < 0$. To find $\bar{x}(\infty)$ we write

$$\bar{x}(\infty) = -\frac{1}{\sigma_o \sqrt{2\pi}} \int_{-\infty}^{o} \exp\left[-\left(\frac{x_o - \bar{x}_o}{\sigma_o \sqrt{2}}\right)^2\right] dx_o + \frac{1}{\sigma_o \sqrt{2\pi}} \int_{o}^{\infty} \exp\left[-\left(\frac{x_o - \bar{x}_o}{\sigma_o \sqrt{2}}\right)^2\right] dx_o .$$

(4.8)

By replacing x_o by $(-x_o)$ in the first integral, it is straightforward to calculate each of the integrals. We get

$$\bar{x}(\infty) = \operatorname{erf}\left(\frac{\bar{x}_o}{\sigma_o \sqrt{2}}\right). \quad (4.9)$$

It is thus seen that in this case where we have two asymptotic states in the deterministic equations, we have an asymptotic state of the stochastic dynamic problem different from any one of the deterministic asymptotic states. As long as σ_o is small compared to $\bar{x}_o$, i.e. when $\bar{x}_o / (\sigma_o\sqrt{2})$ is large and $\bar{x}_o$ is positive, $\bar{x}(\infty)$ will differ only slightly from unity. Similarly, when $\bar{x}_o / (\sigma_o\sqrt{2})$ is numerically large and $\bar{x}_o$ is negative, $\bar{x}(\infty)$ will be very close to -1. In other cases, there are larger differences. As an example, if $\bar{x}_o = \sigma_o = 0.5$, we find $\bar{x}(\infty) = 0.68$.

To compute the second moment, we consider first the integral:

$$m_2(t) = \frac{1}{\sigma_o\sqrt{2\pi}} \int_{-\infty}^{+\infty} \frac{x_o^2}{\alpha x_o^2 + 1 - \alpha} \, e^{-\left(\frac{x_o - \bar{x}_o}{\sigma_o\sqrt{2}}\right)^2} dx_o \, . \qquad (4.10)$$

For $t \to \infty$, $\alpha \to 1$ we find that $m_2(\infty) = 1$ and therefore that

$$\sigma(\infty) = \left(1 - \operatorname{erf}^2\left(\frac{\bar{x}_o}{\sigma_o\sqrt{2}}\right)\right)^{\frac{1}{2}} \qquad (4.11)$$

indicating that $\sigma(\infty)$ is very close to zero if $\bar{x}_o / (\sigma_o\sqrt{2})$ is large. Using the above example, we get for $\bar{x}_o = \sigma_o = 0.5$ that $\sigma(\infty) = 0.73$.

We shall next turn our attention to the time dependent problem. The evaluation of (4.7) is done by the transformation (3.19) leading to

$$\bar{x}(t) = \frac{1}{\sqrt{\pi}} \int_{-\infty}^{+\infty} \frac{\bar{x}_o + \sigma_o \sqrt{2}\xi}{\left[\alpha(\bar{x}_o + \sigma_o \sqrt{2}\xi)^2 + (1-\alpha)\right]^{\frac{1}{2}}} \; e^{-\xi^2} \; d\xi \qquad (4.12)$$

while $m_2(t)$ becomes

$$m_2(t) = \frac{1}{\sqrt{\pi}} \int_{-\infty}^{+\infty} \frac{(\bar{x}_o + \sigma_o \sqrt{2}\xi)^2}{\alpha(\bar{x}_o + \sigma_o \sqrt{2}\xi)^2 + 1 - \alpha} \; e^{-\xi^2} \; d\xi \; . \qquad (4.13)$$

Since it has been impossible for the author to find analytical expressions for the integrals (4.12) and (4.13) in the general case, we must use numerical methods. Integrals of this type are most conveniently evaluated using the approximations using the properties of the Hermite polynomials. A direct evaluation of (4.12) and (4.13) can be performed for the special case $\bar{x}_o = 0$. We find that $\bar{x}(t) = 0$ for all t, while

$$m_2(t) = \sigma(t)^2 = \frac{1}{\alpha}\left\{1 - \sqrt{\pi}.\beta.\; e^{\beta^2}\left(1 - \mathrm{erf}(\beta)\right)\right\}. \qquad (4.14)$$

(4.14) will be used later in order to make a comparison with a closure solution.

We are next going to consider the problem using the probability density function (2.6) and thereby restrict the variable x to the positive domain. The following integral must be evaluated:

$$\bar{x}(t) = \int_{o}^{\infty} \frac{x_o}{(\alpha x_o^2 + 1 - \alpha)^{\frac{1}{2}}} \; \frac{1}{\beta^p \, \Gamma(p)} \; x_o^{p-1} \; e^{-\frac{x_o}{\beta}} \; dx_o \qquad (4.15)$$

The evaluation of (4.15) creates problems for an arbitrary value of p, but if p is a positive integer, we may obtain solutions in a closed form. To accomplish this, we introduce the variable z by

$$x_o = \beta a z, \quad a^2 = \frac{1}{\beta^2} \quad \frac{1-\alpha}{\alpha} \quad . \tag{4.16}$$

We get then

$$\bar{x}(t) = \frac{a^p}{\sqrt{\alpha}\,\Gamma(p)} \int_o^\infty \frac{z^p}{\sqrt{1+z^2}} \; e^{-az} \; dz \quad . \tag{4.17}$$

We note that

$$\int_o^\infty \frac{1}{\sqrt{1+z^2}} \; e^{-az} \; dz = \frac{\pi}{2} \; (H_o(a) - Y_o(a)) \tag{4.18}$$

where $H_o(a)$ is the Struve function and $Y_o(a)$ is the Bessel function of the second kind. The formula (4.18) may be used to evaluate (4.17) for integer values of p. Differentiating (4.18) p times with respect to a, we find

$$\int_o^\infty \frac{z^p}{\sqrt{1+z^2}} \; e^{-az} \; dz = (-1)^p \; \frac{\pi}{2} \left(\frac{d^p H_o(a)}{da^p} - \frac{d^p Y_o(a)}{da^p} \right). \tag{4.19}$$

The main problem is now to express the right hand side of (4.19) in terms of H_o, H_1, Y_o and Y_1 which are tabulated functions. For this purpose, we have the formulas

$$\frac{dH_0}{da} = \frac{2}{\pi} - H_1 \qquad \frac{dY_0}{da} = Y_1(a)$$

$$\frac{dH_1}{da} = H_0 - \frac{1}{a} H_1 \qquad \frac{dY_1}{da} = Y_0 - \frac{1}{a} Y_1 \tag{4.20}$$

Using a step by step procedure, we arrive at the following formulas:

$$p=1: \quad \bar{x}(t) = \frac{a}{\sqrt{\alpha}} \left\{ \frac{\pi}{2} \left(H_1(a) - Y_1(a) \right) - 1 \right\}$$

$$p=2: \quad \bar{x}(t) = \frac{a^2}{\sqrt{\alpha}} \frac{\pi}{2} \cdot \left\{ \frac{1}{a} (H_1 - Y_1) - (H_0 - Y_0) \right\} \tag{4.21}$$

$$p=3: \quad \bar{x}(t) = \frac{1}{2} \frac{a^3}{\sqrt{\alpha}} \left\{ 1 + \frac{\pi}{2} \left[\left(\frac{2}{a^2} - 1 \right) (H_1 - Y_1) - \frac{1}{a} (H_0 - Y_0) \right] \right\}$$

$$p=4: \quad \bar{x}(t) = \frac{1}{6} \frac{a^4}{\sqrt{\alpha}} \left\{ \frac{1}{a} - \frac{\pi}{2} \left(\frac{3}{a^2} - 1 \right) \left[(H_0 - Y_0) - \frac{2}{a} (H_1 - Y_1) \right] \right\}.$$

We note from (4.16) that

$$\alpha^{-1} = 1 + \beta^2 a^2, \quad t = \frac{1}{2} \ln. \left[1 + \frac{1}{\beta^2 a^2} \right] \tag{4.22}$$

(4.21) and (4.22) can be used to calculate $\bar{x}(t)$ in individual cases, and the results can be compared with the results obtained from (4.12) and (4.13). Such comparisons will be made later in this section. The solutions (4.21) satisfy the initial condition that $\bar{x}(0) = \bar{x}_0$. We note that $t = 0$ corresponds to $a \to \infty$. By using the asymptotic expansions

of H_0 - Y_0 and H_1 - Y_1, it is possible to show that the initial condition is satisified in the cases in (4.21). We note also that for $t \to \infty$, i.e. $a = 0$, it holds that $\bar{x}(\infty) = 1$.

To calculate the second moment, we need to evaluate

$$m_2(t) = \int_0^\infty \frac{x_0^2}{\alpha x_0^2 + 1 - \alpha} \cdot \frac{1}{\beta^p \Gamma(p)} \cdot x_0^{p-1} e^{-\frac{x_0}{\beta}} dx_0 . \quad (4.23)$$

Using the same transformation as before we get

$$m_2(t) = \frac{a^p}{\alpha \Gamma(p)} \int_0^\infty \frac{z^{p+1}}{1+z^2} e^{-az} dz . \quad (4.24)$$

The following two integrals are known:

$$\int_0^\infty \frac{z^{2n+1}}{1+z^2} e^{-az} dz = (-1)^{n-1} \left[Ci(a) \cos a + (Si(a) - \frac{\pi}{2}) \sin a \right] + \frac{1}{a^{2n}} \sum_{k=1}^{n} (2n-2k+1)!(-a^2)^{k-1} \quad (4.25)$$

and

$$\int_0^\infty \frac{z^{2n}}{1+z^2} e^{-az} dz = (-1)^n \left[Ci(a) \sin a - (Si(a) - \frac{\pi}{2}) \cos a \right] + \frac{1}{a^{2n-1}} \sum_{k=1}^{\infty} (2n-2k)!(-a^2)^{k-1} \quad (4.26)$$

where Ci(a) and Si(a) are the standard notations for the cosine and sine integrals (Gradshteyn & Ryzhik, 1965). Using these integrals, we list the following results for specific values of p:

$$
\begin{aligned}
p=1: \quad & m_2 = \alpha^{-1} a \left[a^{-1} - \mathrm{Ci}(a) \sin a + (\mathrm{Si}(a) - \tfrac{\pi}{2}) \cos a \right] \\
p=2: \quad & m_2 = \alpha^{-1} a^2 \left[a^{-2} + \mathrm{Ci}(a) \cos a + (\mathrm{Si}(a) - \tfrac{\pi}{2}) \sin a \right] \\
p=3: \quad & m_2 = \tfrac{1}{2}\alpha^{-1} a^3 \left[a^{-3}(2-a^2) + \mathrm{Ci}(a) \sin a - (\mathrm{Si}(a) - \tfrac{\pi}{2}) \cos a \right] \\
p=4: \quad & m_2 = \tfrac{1}{6}\alpha^{-1} a^4 \left[a^{-4}(6-a^2) - \mathrm{Ci}(a) \cos a - (\mathrm{Si}(a) - \tfrac{\pi}{2}) \sin a \right]
\end{aligned}
\tag{4.27}
$$

From the formulas in (4.27) it is possible to show that the initial condition is satisfied by using the asymptotic expansions, and it can also be shown that $\lim_{t\to\infty} m_2(t) = 1$. It is thus evident that $\lim_{t\to\infty} \sigma_2(t) = 0$.

Comparing the results using the Pearson probability density function with those obtained from the Gaussian probability density function, we can conclude that in the former case (equations (4.15) to (4.27)) we find an asymptotic behaviour similar to the case treated in Sections 2 and 3. For large values of time $\bar{x}(t)$ will approach unity just as the deterministic solution while the limiting value of $\sigma(t)$ is zero. Using the Gaussian function, the results show (see (4.9) and (4.11)) that $\bar{x}(t)$ and $\sigma(t)$ deviate significantly from unity and zero for large values of t if the initial uncertainty σ_o is large compared to the initial value of $\bar{x}$.

This behaviour is due to the fact that two asymptotic states exist in the full domain from $-\infty$ to $+\infty$ used in the Gaussian case while only one such state can be recognised in the Pearson case.

We shall finally consider the problem using the same closure assumption as in Section 3. Referring to the procedure established by (3.1) we apply the operator E to (4.1) assuming that μ_3 and μ_4 vanish, we get:

$$\frac{d\bar{x}}{dt} = \bar{x} - \bar{x}^3 - 3\bar{x}\mu \qquad (4.28)$$

setting $\mu_2 = \mu$. The expression for the rate of change of μ is found by noting that

$$\frac{d\mu}{dt} = E\left(2x \frac{dx}{dt}\right) - 2\bar{x} \frac{d\bar{x}}{dt} \qquad (4.29)$$

Substituting from (4.1) and (4.28) in (4.29) we get

$$\frac{d\mu}{dt} = 2\mu (1 - 3\bar{x}^2) \qquad (4.30)$$

The system (4.28) and (4.30) form a closed system due to our closure assumption. It has not been possible to obtain general solutions to the system. Some numerical solutions will be presented later. It can, however, be seen that the system (4.28), (4.30) has stationary states not found in the general exact solution. We note that $x = \pm \sqrt{3}/3$ and $\mu = 2/9$

are such stationary states. In addition, the system has the stationary states $\mu = 0$ and $\bar{x} = \pm 1$ corresponding to the deterministic equation. Of these four steady states, we find by linearising (4.28) and (4.30) that the first two states $(\pm \sqrt{3}/3,\ 2/9)$ are unstable while the other two $(\pm 1,\ 0)$ are stable. It is therefore understandable that the behaviour of the solutions of the system (4.28), (4.30) will deviate very much from the exact solution if the initial state is close to the unstable steady state. As an example, we select an initial state $\bar{x}_0 = 0.5$, $\mu_0 = 0.25$ deviating slightly from the steady state $\bar{x}_0 = 0.57735$, $\mu_0 = 0.22222$. The solution, obtained numerically from (4.28), (4.30) by the Runge-Kutta method, is shown in Figures 5a and 5b. $\bar{x}(t)$ decreases rapidly from 0.5 to 0, $\mu(t)$ increases very slowly at first ($t < 2$), but at the time when $\bar{x}(t)$ becomes zero, $\mu(t)$ increases very rapidly. This behaviour is understandable from the system (4.28), (4,30) because if $\bar{x}$ becomes zero it will according to (4.28) stay zero. μ will at the same time be governed by the equation

$$\frac{d\mu}{dt} = 2\mu \tag{4.31}$$

which indicates an exponential growth, i.e.

$$\mu = \mu_* \, e^{2(t-t_*)} \tag{4.32}$$

where μ_* is the value of μ, when $\bar{x} = 0$, and t_* is the time at which $\bar{x} = 0$. When the curve (4.32) is plotted with $t_* = 2.6$ and $\mu_* = 8.72$, we find agreement with the curve in Figure 5b for $t \geq 2.6$.

We shall finally give some examples of calculations based on (4.12), (4.13), on (4.21), (4.27) and on (4.28), (4.30). These examples have been selected in such a way that (4.21) and (4.27) can be applied, i.e. for small integer values of p. The results show the influence of the probability density function and the closure assumption.

Figures 6a and 6b show the case with initial conditions $\bar{x}_0 = 2$, $\sigma_0^2 = 1$. It is seen that all three calculations agree with each other for small values of t. However, as t becomes larger, the curve $\bar{x} = \bar{x}(t)$ based on the Gaussian probability density deviates more and more and approaches, for large t, a value less than unity in agreement with (4.9). A similar deviation is found for $\mu = \mu(t)$ as displayed in Fig. 6b where the curve based on the Gaussian function, in the limit for large t, approaches a value different from zero. Figures 7a and 7b show the case $\bar{x}_0 = 0.5$, $\sigma_0^2 = 0.125$. In this case, we find a somewhat larger deviation between the curves based on the closure scheme and the Pearson distribution, while the curves based on the Gaussian distribution deviate considerably from the other two.

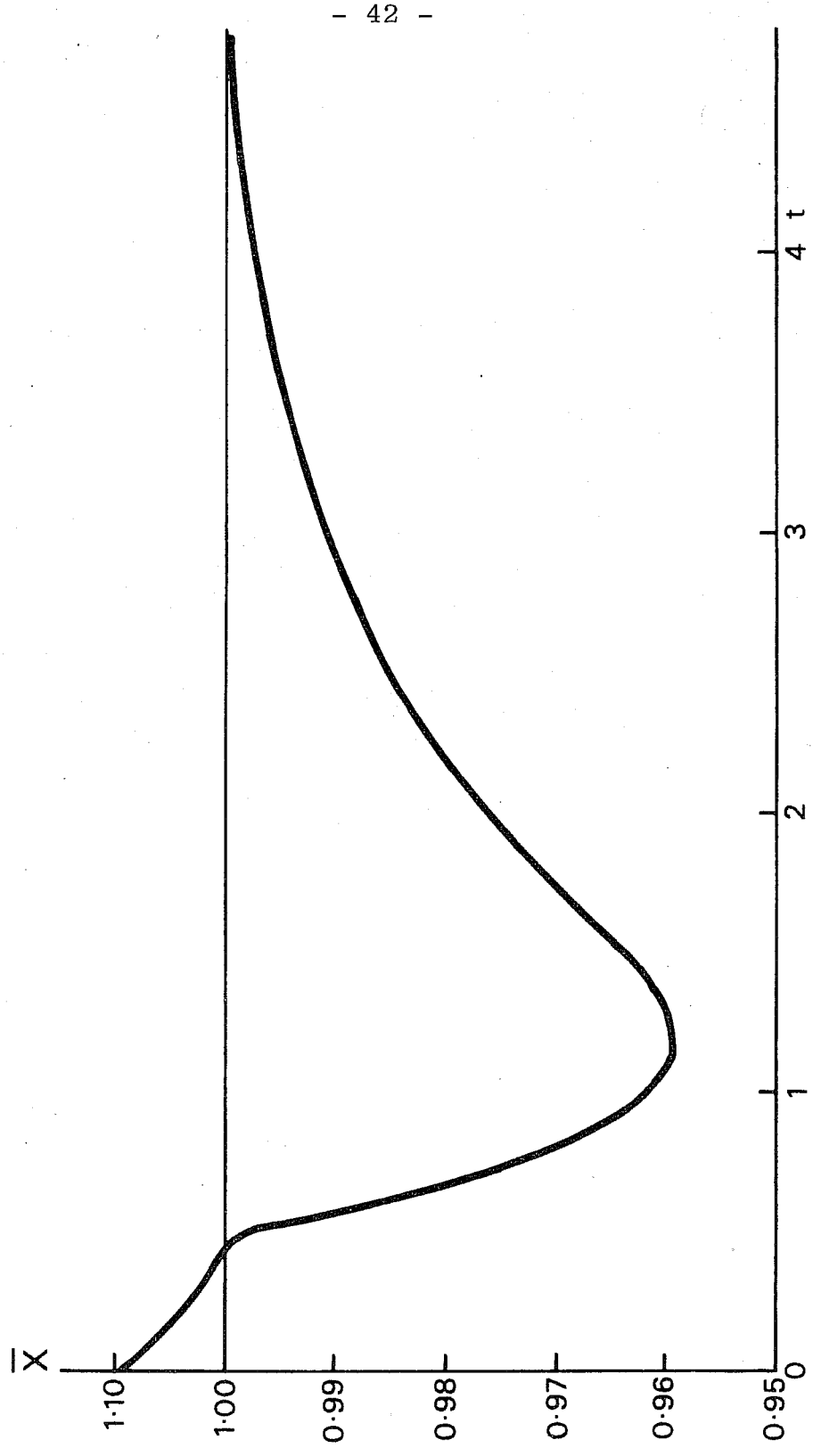

Fig. 4 : $x = x(t)$ computed from (3.24) with $x = 1.1$, $\sigma = 0.5$.

5. Monte Carlo calculations

The calculations presented in the previous sections show clearly that the solution given in (2.5) can be applied only when $x(x_o,t)$ is known in an analytical form. This is generally not the case. One method to use is then to introduce a closure assumption as described in Sections 3 and 4. However, it is obvious that this approach will lead to very time consuming calculations in applications as has been demonstrated by Pitcher (1977) who applied the stochastic dynamic method to short-range weather predictions. Another approach is to replace the stochastic dynamic forecast procedure by a finite sample of deterministic forecasts from different initial states. Such a Monte Carlo technique has in the meteorological context been analysed by Leith (1974).

The use of the Monte Carlo technique requires a sample of initial states. From each of these a deterministic forecast is made. At any given time one may use the sample of forecasts to obtain the most likely forecast and the uncertainty connected with this forecast by suitable statistical methods. An average and a standard deviation computed from the available sample of forecasts is normally a minimum requirement. In using the Monte Carlo technique at least two questions arise. The first is if the process leads to convergence for a sufficiently large initial sample. It has been assumed in previous calculations that this is the case. The second question is how many elements we need to have in the initial sample to obtain a reliable estimate of the average and the standard deviation during the forecast

period. There is clearly no unique answer to this question because the answer will depend on the forecast period and the physical nature of the problem. However, for the short-range meteorological problem, Leith (1974) has determined that "a Monte Carlo forecasting procedure represents a practical computable approximation to the stochastic dynamic forecasts" and that adequate accuracy should be obtained with sample sizes as small as 8.

We shall use the model described in Section 4 to explore some of the problems which will arise in applying the Monte Carlo technique on a long time scale. Assuming that we consider initial states in the interval from $-\infty$ to $+\infty$, we know that a positive initial state will result in a forecast which at large times will approach +1 while a negative initial state under the same conditions will approach -1. It is thus clearly of importance to know if the initial state, characterised by a mean value $\bar{x}_o$ and a standard deviation σ_o, with a high degree of certainty is in the positive or the negative domain. For example, if $\bar{x}_o = 2$ and $\sigma_o = 0.1$, it is highly unlikely that any negative element should be in the initial sample, but on the other hand, if $\bar{x}_o = 0.5$ and $\sigma_o = 0.5$, we must include both positive and negative elements in the initial sample. To explore the implications of these very different situations, we consider first the initial states. In Appendix 3 it is shown how one can construct a sample of N equidistant points having a given mean value $\bar{x}_o$ and a given standard deviation σ_o. We may use the procedure to calculate a few examples.

Figure 8a shows x_A, the average x, as a function of time for the case $\bar{x}_o = 2$, $\sigma_o = 0.5$ and for a sample of 5 and 21 initial points. It is seen that the two cases coincide for all practical purposes. This is understandable because the initial sample contains only points with a positive value of x_o, and the curves for each of these points will approach +1 for large values of the time. Figure 8b shows that a similar statement can be made for $\sigma_A(t)$. From this and other calculations we conclude that relatively few points are necessary in the initial sample if all of the initial states lead to the same asymptotic state.

We consider next the case $x_o = 0.5$, $\sigma_o = 0.5$. In this case the initial sample will contain some elements with a negative value of x_o and therefore an asymptotic state of -1. As shown in Section 4 (see eg. (4.9) and (4.11) we expect asymptotic states of $\bar{x}$ and σ between -1 and +1 in these cases. In the particular example chosen here we have $\bar{x}(\infty) = 0.68$ and $\sigma(\infty) = 0.73$. Figure 9 shows $\bar{x}_A(t)$ for initial sample sizes of 3, 5, 7, .., 13 points. It is seen that while the curves coincide well for small values of t, there are large differences at large values of t. We can explain this behaviour by finding $\bar{x}_A(\infty)$ for a number of sample sizes. The procedure is very simple. All we need to know is how many positive and negative initial states we have in the sample. Each of the positive states will approach +1 and the negative states will approach -1 for $t \to \infty$. From the formula given in Appendix 3, we can get this information. On the basis of this procedure we have constructed the following table.

Table 1

The values $\bar{x}_A(\infty)$ and $\bar{\sigma}_A(\infty)$ as a function of sample size.

N	$\bar{x}_A(\infty)$	$\bar{\sigma}_A(\infty)$
3	0.3333	0.9428
5	0.6000	0.8000
7	0.5714	0.7285
9	0.5556	0.8315
11	0.6364	0.7714
13	0.5385	0.8426
15	0.6000	0.8000
17	0.5294	0.8484
19	0.5789	0.8154
21	0.6190	0.7854
23	0.5652	0.8249
25	0.6000	0.8000
27	0.5556	0.8315

The table indicates that neither the values of $\bar{x}_A(\infty)$ nor those of $\bar{\sigma}_A(\infty)$ approach a limiting value for the relatively small values of N, the sample size included in the list. The curves $\bar{x}_A(t)$ and $\bar{\sigma}_A(t)$ are shown in Figure 10, a and b respectively, for N = 5 and N = 21. We note the good agreement for small t and the large disagreement for large t. The question is if the Monte Carlo procedure is convergent, and if so, what the limiting value is. We note first of all that if all the initial values of the sample are of one sign the process is rapidly converging to +1 if they are positive and -1 if they are negative. The remaining problem is therefore the case in which the initial sample contains both positive

and negative elements. From Appendix 3 we note that a sample of (2m+1) points may be written in the form:

$$x(k) = \bar{x}_o - md + (k-1)d, \quad k = 1, 2, \ldots\ldots, (2m+1). \tag{5.1}$$

If the set (5.1) contains negative elements, they are characterised by $k < k_*$ where

$$k_* = < 1 + m - \frac{\bar{x}_o}{d} > \tag{5.2}$$

where $< >$ means the integer part of k_*.

Using (A.26) for d, we get

$$k_* = < 1 + m - \frac{\bar{x}_o}{\sigma_o\sqrt{3}} \sqrt{m(m+1)} > \tag{5.3}$$

Each of these negative elements will converge to -1 for $t \to \infty$ while positive elements will converge to +1. The average value of x at infinity is therefore:

$$\bar{x}(\infty) = \frac{(2m+1) - 2k_*}{(2m+1)} \tag{5.4}$$

(5.4) reproduces the numbers in the table except for the case m = 3 (N = 7) because this special case includes x = 0 in the sample. From (5.4) combined with (5.3) we find that the limiting value of $\bar{x}(\infty)$ when $m \to \infty$ is

$$\bar{x}(\infty) = \frac{\bar{x}_0}{\sigma_0\sqrt{3}} \qquad (5.5)$$

The Monte Carlo procedure is therefore convergent, and in our special case $\bar{x}_0 = 0.5$, $\sigma_0 = 0.5$, we find that $\bar{x}(\infty) = 0.5774$ when the sample becomes infinitely large.

We note from (5.4) and (5.5) that quite large sample sizes are necessary to obtain a good approximation to the value given in (5.5). In addition, it is seen that the limiting value in the Monte Carlo procedure, with the design of the sample as given in Appendix 3, will be different from both the limiting values obtained from the two probability density functions used in Section 4. Such a result is to be expected because the Monte Carlo sample is restricted to the region $\bar{x}_0 - \sigma_0\sqrt{3} < x < \bar{x}_0 + \sigma_0\sqrt{3}$ in the limit while the probability density functions cover either the region $o < x < \infty$ or $-\infty < x < +\infty$.

The main result from this section is therefore that the Monte Carlo procedures will work very well and approach the desired limiting value if the elements in the initial sample belong to the subset having the same asymptotic state. If the initial sample contains elements from subsets leading to different asymptotic values, the Monte Carlo procedure will still be convergent but the limiting value will be between the asymptotic states for the deterministic problem.

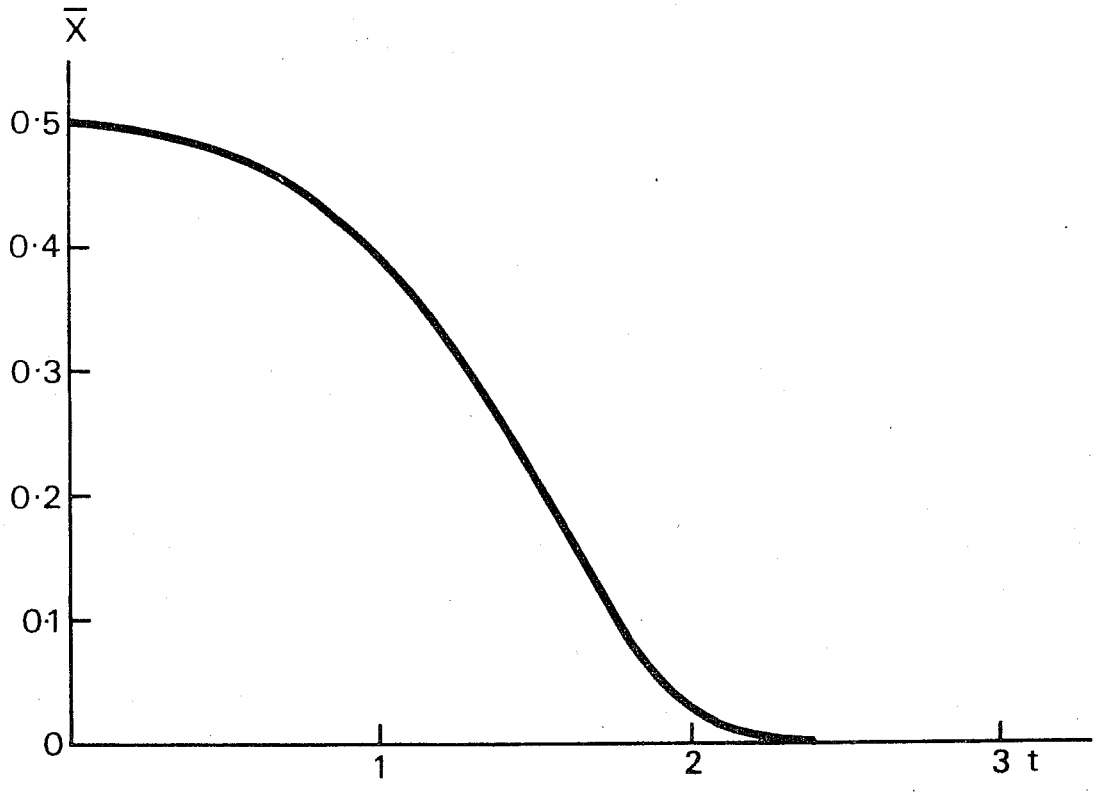

Fig. 5a : $\bar{x} = \bar{x}(t)$ computed from (4.28) and (4.30) by numerical integration with inital conditions $\bar{x}_0 = 0.5$, $\sigma_0 = 0.5$, i.e. $\mu_0 = 0.25$.

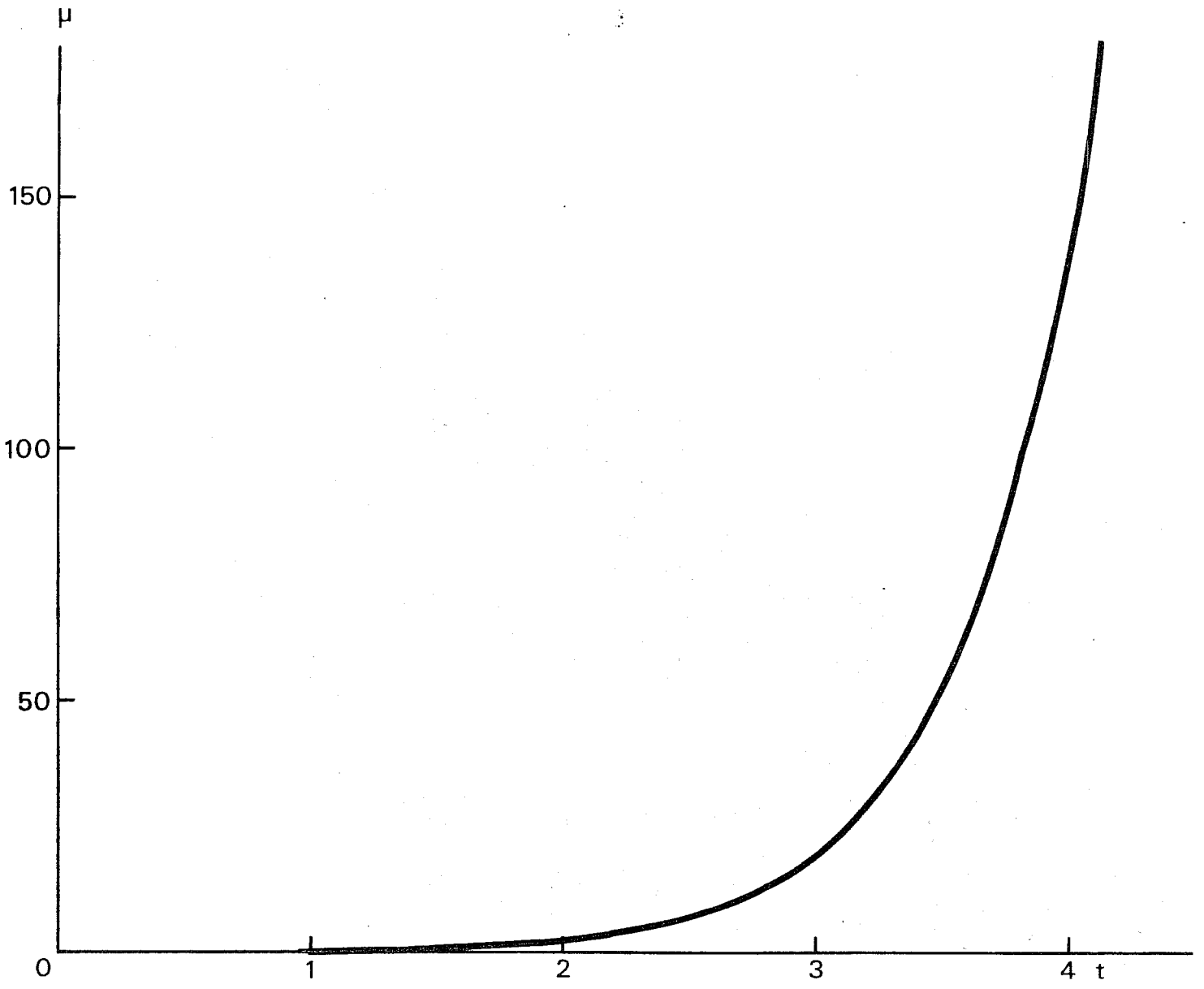

Fig. 5b : $\mu = \mu(t)$ computed from (4.28) and (4.30) by numerical integration with initial conditions $x = 0.5$, $\mu = 0.25$.

6. A simple meteorological example

Some years ago the author (Wiin-Nielsen, 1975) considered some aspects of a simple meteorological model based on the advection equation

$$\frac{\partial u}{\partial t} + u \frac{\partial u}{\partial x} = 0 \quad . \tag{6.1}$$

This equation was transformed into the spectral domain and the resulting infinite set of ordinary differential equations was truncated in wave number space. Considering the two largest components only and denoting the amplitudes by x(t) and y(t), we get the following coupled differential equations:

$$\frac{dx}{dt} = \tfrac{1}{2} xy \ ,$$

$$\frac{dy}{dt} = -\tfrac{1}{2} x^2 \ . \tag{6.2}$$

The "kinetic energy" $x^2 + y^2$ is conserved and it is convenient to set

$$x_o^2 + y_o^2 = R_o^2 \ . \tag{6.3}$$

The solution to (6.2) is then

$$x = \frac{x_o R_o}{\cos h\ (\frac{1}{2}R_o t)} \cdot \frac{1}{R_o - y_o \tan h\ (\frac{1}{2}R_o t)} \quad , \qquad (6.4)$$

and

$$y = R_o \frac{y_o - R_o \tan h\ (\frac{1}{2}R_o t)}{R_o - y_o \tan h\ (\frac{1}{2}R_o t)} \quad . \qquad (6.5)$$

The stochastic dynamic solution can be obtained by using the generalisation of (2.6) and (2.7) to two dimensions. Specifically,

$$\bar{x}(t) = \frac{1}{2\pi\sigma_1\sigma_2} \int_{-\infty}^{+\infty}\int_{-\infty}^{+\infty} \frac{x_o}{\cos h\ (\frac{1}{2}R_o t)} \cdot \frac{R_o}{R_o - y_o \tan h\ (\frac{1}{2}R_o t)}$$

$$\exp\left[-\left(\frac{x_o - \bar{x}_o}{\sigma_1\sqrt{2}}\right)^2 - \left(\frac{y_o - \bar{y}_o}{\sigma_2\sqrt{2}}\right)^2\right] dx_o\, dy_o \quad , \qquad (6.6)$$

$$(t) = \frac{1}{2\pi\sigma_1\sigma_2} \int_{-\infty}^{+\infty}\int_{-\infty}^{+\infty} R_o \frac{y_o - R_o \tan h\ (\frac{1}{2}R_o t)}{R_o - y_o \tan h\ (\frac{1}{2}R_o t)} \exp\left[-\left(\frac{x_o - \bar{x}_o}{\sigma_1\sqrt{2}}\right)^2 - \left(\frac{y_o - \bar{y}_o}{\sigma_2\sqrt{2}}\right)^2\right] dx_o\, dy_o \quad .$$

Setting

$$x_o = \bar{x}_o + \sigma_1\sqrt{2}\xi, \qquad y_o = \bar{y}_o + \sigma_2\sqrt{2}\eta \tag{6.7}$$

we may write:

$$\bar{x}(t) = \frac{1}{\pi}\int_{-\infty}^{+\infty}\int_{-\infty}^{+\infty} F(\xi,\eta)\, e^{-(\xi^2+\eta^2)}\, d\xi d\eta \tag{6.8}$$

and

$$\bar{y}(t) = \frac{1}{\pi}\int_{-\infty}^{+\infty}\int_{-\infty}^{+\infty} G(\xi,\eta)\, e^{-(\xi^2+\eta^2)}\, d\xi d\eta \tag{6.9}$$

where

$$F(\xi,\eta) = \frac{\bar{x}_o + \sigma_1\sqrt{2}\xi}{\cos h(\frac{1}{2}R_o t)} \quad \frac{R_o}{R_o - (\bar{y}_o + \sigma_2\sqrt{2}\eta)\tan h(\frac{1}{2}R_o t)} \tag{6.10}$$

and

$$G(\xi,\eta) = R_o \frac{(\bar{y}_o + \sigma_2\sqrt{2}\eta) - R_o \tan h(\frac{1}{2}R_o t)}{R_o - (\bar{y}_o + \sigma_2\sqrt{2}\eta)\tan h(\frac{1}{2}R_o t)} \tag{6.11}$$

$$R_o(\xi,\eta) = \left[(\bar{x}_o + \sigma_1\sqrt{2}\xi)^2 + (\bar{y}_o + \sigma_2\sqrt{2}\eta)^2\right]^{\frac{1}{2}} \tag{6.12}$$

It is seen that the integrals (6.8) and (6.9) are well defined because the denominator is always different from zero. This is due to the fact that tan h $(\frac{1}{2}R_o t)$ is always less than unity and $y_o < R_o$. The numerical evaluation of

(6.8) and (6.9) is therefore straightforward using the integration method recommended by Pitcher (1974). We may also use analogous procedures to calculate the second (or higher) moments. We have:

$$\mu_{10}(t) = \frac{1}{\pi}\int_{-\infty}^{+\infty}\int_{-\infty}^{+\infty} F(\xi,\eta)^2 \, e^{-(\xi^2+\eta^2)} \, d\xi d\eta - \bar{x}(t)^2 \qquad (6.13)$$

$$\mu_{01}(t) = \frac{1}{\pi}\int_{-\infty}^{+\infty}\int_{-\infty}^{+\infty} G(\xi,\eta)^2 \, e^{-(\xi^2+\eta^2)} \, d\xi d\eta - \bar{y}(t)^2 \qquad (6.14)$$

$$\mu_{11}(t) = \frac{1}{\pi}\int_{-\infty}^{+\infty}\int_{-\infty}^{+\infty} F(\xi,\eta)\, G(\xi,\eta) \, e^{-(\xi^2+\eta^2)} \, d\xi d\eta - \bar{x}(t)\bar{y}(t) \qquad (6.15)$$

The calculated values of μ_{10}, μ_{01} and μ_{11} can at any fixed time be used to construct the uncertainty ellipse according to the procedure given in Appendix 2.

The exact solution given above may be compared with a solution obtained through a closure approximation. We shall use the same closure as in Section 2, i.e. the neglect of third and higher moments. Starting from (6.2) we find

$$\frac{d\bar{x}}{dt} = -\frac{1}{2}\bar{x}\,\bar{y} + \frac{1}{2}\mu_{11}$$

$$\frac{d\bar{y}}{dt} = -\frac{1}{2}\bar{x}^2 - \frac{1}{2}\mu_{10}$$

$$\frac{d\mu_{10}}{dt} = \bar{x}\,\mu_{11} + \bar{y}\,\mu_{10} \tag{6.16}$$

$$\frac{d\mu_{01}}{dt} = -2\bar{x}\,\mu_{11}$$

$$\frac{d\mu_{11}}{dt} = \frac{1}{2}\,\bar{x}\,\mu_{01} + \frac{1}{2}\,\bar{y}\,\mu_{11} - \bar{x}\,\mu_{10}$$

The system (6.16) may be integrated numerically. Since we calculate μ_{10}, μ_{01} and μ_{11} as a function of time, we may also in this case construct the uncertainty ellipses.

It is of interest to find the asymptotic state to which the system described by (6.6) will arrive for large values of t. We note that $\bar{x}(\infty) = 0$ from the first expression in (6.6). $\bar{y}(\infty)$ is determined by the integral

$$\bar{y}(\infty) = \frac{-1}{2\pi\sigma_1\sigma_2}\int_{-\infty}^{\infty}\int_{-\infty}^{\infty} R_o \exp\left[-\left(\frac{x_o-\bar{x}_o}{\sigma_1\sqrt{2}}\right)^2 - \left(\frac{y_o-\bar{y}_o}{\sigma_2\sqrt{2}}\right)^2\right] dx_o\, dy_o \tag{6.17}$$

From (6.5) we note that $y(\infty) = -R_o$. It is to be expected that $\bar{y}(\infty)$ will differ from $y(\infty)$ because of the uncertainty in the initial state. We need thus to calculate the integral in (6.17). To do this we introduce new variables as follows:

$$x_o = \sigma_o \sqrt{2}\, x, \quad y_o = \sigma_o \sqrt{2}\, y, \quad \bar{x}_o = \sigma_o \sqrt{2}\, \bar{x}, \quad \bar{y}_o = \sigma_o \sqrt{2}\, \bar{y}$$

(6.18)

where we have further assumed that $\sigma_1 = \sigma_2 = \sigma_o$.

With this transformation we find

$$\bar{y}(\infty) = -\frac{\sigma_o \sqrt{2}}{\pi} \int_{-\infty}^{+\infty} \int_{-\infty}^{+\infty} \sqrt{x^2+y^2}\, \exp\left[-(x-\bar{x})^2 - (y-\bar{y})^2 \right] dxdy.$$

(6.19)

In (6.19) we introduce polar coordinates as follows:

$$x = r \cos\phi, \quad y = r \sin\phi, \quad \bar{x} = \bar{r} \cos\bar{\phi}, \quad \bar{y} = \bar{r} \sin\bar{\phi}$$

(6.20)

and we get

$$\bar{y}(\infty) = -\frac{\sigma_o \sqrt{2}}{\pi}\, e^{-\bar{r}^2} \int_o^\infty \left[r^2\, e^{-r^2} \left\{ \int_o^{2\pi} e^{2\bar{r}r \cos(\phi-\bar{\phi})}\, d\phi \right\} \right] dr.$$

(6.21)

The inner integral in (6.21) is well known because

$$\int_o^{2\pi} e^{2\bar{r}r \cos(\phi-\bar{\phi})}\, d\phi = 2 \int_o^{\pi} e^{2\bar{r}r \cos\theta}\, d\theta = 2\pi I_o(2\bar{r}r)$$

(6.22)

where I_o is the modified Bessel function. We have

therefore

$$\bar{y}(\infty) = -\sigma_o 2\sqrt{2}\, e^{-\bar{r}^2} \int_o^\infty r^2\, I_o(2\bar{r}r)\, e^{-r^2}\, dr \qquad (6.23)$$

The integral in (6.23) may be evaluated by noting that

$$I_o(2\bar{r}r) = J_o(2\bar{r}ir) \qquad (6.24)$$

where J_o is the ordinary Bessel function of order zero. According to Gradshteyn and Ryzhik (1965) we find that

$$\bar{y}(\infty) = -\sigma_o\sqrt{2}\, e^{-\bar{r}^2}\, \Gamma(\tfrac{3}{2})\, M(\tfrac{3}{2},\ 1,\ \bar{r}^2) \qquad (6.25)$$

where M is the confluent hypergeometric function. (6.25) can be evaluated from standard tables.

It is also possible to obtain a formula for $\mu_{01}(\infty)$. We start by calculating

$$m_2(\infty) = \frac{1}{2\pi\sigma_o{}^2} \int_{-\infty}^{+\infty}\int_{-\infty}^{+\infty} (x_o{}^2+y_o{}^2)\, e^{-\left[\left(\frac{x_o-\bar{x}_o}{\sigma_o\sqrt{2}}\right)^2+\left(\frac{y_o-\bar{y}_o}{\sigma_o\sqrt{2}}\right)^2\right]} dx_o\, dy_o \qquad (6.26)$$

Using the transformations (6.18) and (6.20) we may write (6.26) in the form

$$m_2(\infty) = 4\sigma_o{}^2\, e^{-\bar{r}^2} \int_o^\infty r^3\, I_o(2\bar{r}r)\, e^{-r^2}\, dr \qquad (6.27)$$

which can be integrated to

$$m_2(\infty) = 2\sigma_o^2 \, e^{-\bar{r}^2} \, M(2,1,\bar{r}^2) \qquad (6.28)$$

Since (6.28) can be obtained from the tables of the hypergeometric function, we can also calculate

$$\mu_{01}(\infty) = m_2(\infty) - \bar{y}(\infty)^2 \qquad (6.29)$$

Based on the results in (6.25) and (6.29), we may take a further step and calculate the third moment. Such a calculation will at least give an answer to how large the third moment is in the asymptotic state. We start by calculating the integral

$$m_3(\infty) = -\frac{1}{2\pi\sigma_o^2} \int_{-\infty}^{+\infty}\int_{-\infty}^{+\infty} (x_o^2+y_o^2)^{\frac{3}{2}} \; e^{-\left[\left(\frac{x_o-\bar{x}_o}{\sigma_o\sqrt{2}}\right)^2 + \left(\frac{y_o-\bar{y}_o}{\sigma_o\sqrt{2}}\right)^2\right]} dx_o dy_o \qquad (6.30)$$

which, using the transformations (6.18) and (6.20) becomes

$$m_3(\infty) = -2(2\sigma_o^2)^{\frac{3}{2}} \, e^{-\bar{r}^2} \int_o^\infty r^4 \, I_o(2\bar{r}r) \, e^{-r^2} \, dr \qquad (6.31)$$

A further evaluation of (6.31) leads to

$$m_3(\infty) = -(2\sigma_o^2)^{\frac{3}{2}} \, \Gamma(\tfrac{5}{2}) \, e^{-\bar{r}^2} \, M(\tfrac{5}{2}, 1, \bar{r}^2) \qquad (6.32)$$

With this result we may finally calculate

$$\mu_3(\infty) = m_3(\infty) - 3\bar{y}(\infty)\,\mu_{01}(\infty) - \bar{y}(\infty)^3 \qquad (6.33)$$

In computing the values in the following table, it was assumed that $\bar{x}_0^2+\bar{y}_0^2 = 1$. We find then that

$$\bar{r}^2 = (2\sigma_0^2)^{-1} \qquad (6.34)$$

The results have therefore been listed as a function of σ_0 which furthermore has been restricted to values less than unity. σ_0 is a measure of the initial uncertainty. We note that the asymptotic values $\sigma_{01}(\infty) = \mu_{01}(\infty)^{\frac{1}{2}}$ of the uncertainty are less than the initial uncertainty in our example. The asymptotic position is $(\bar{x}(\infty),\ \bar{y}(\infty))$ of which $\bar{x}(\infty) = 0$. The table shows that $\bar{y}(\infty)$ is numerically larger than unity while a deterministic calculation gives $y(\infty) = 1$. The coefficient of skewness of the distribution, defined as

$$S = \frac{\mu_3}{\mu_{01}^{\frac{3}{2}}} \qquad (6.35)$$

and computed in the table shows that the neglect of the third moment in the approximate calculation is justified when the initial uncertainty is sufficiently small.

Table 2

Table of asymptotic values of $\bar{y}$, σ_{01}, μ_3 and s as a function of σ_o with $\bar{x}_o^2 + \bar{y}_o^2 = 1$.

σ_o	$\bar{y}(\infty)$	$\sigma_{01}(\infty)$	$\mu_3(\infty)$	$s(\infty)$
1.0000	- 1.55	0.8324	- 0.81027	- 1.405
0.7071	- 1.28	0.5972	- 0.08155	- 0.383
0.5000	- 1.14	0.4572	- 0.02005	- 0.210
0.4082	- 1.09	0.3861	- 0.00693	- 0.120
0.3536	- 1.07	0.3400	- 0.00293	- 0.075
0.3162	- 1.05	0.3070	- 0.00141	- 0.049
0.2500	- 1.03	0.2457	- 0.00030	- 0.020
0.2236	- 1.02	0.2206	- 0.00013	- 0.012

The above analytical results can be used to compare an integration based on the system (6.16) which is the approximate stochastic-dynamic equation with the closure assumption that third and higher moments vanish with the exact results for very large values of time. The system (6.16) was therefore integrated numerically using a Runge-Kutta approximation for the time derivations. The integration was continued until an asymptotic state was reached. We note from (6.16) that a steady state is characterized by $\bar{x} = 0$, $\mu_{10} = 0$ and $\mu_{11} = 0$. It is furthermore seen that the following quantity is conserved

$$\bar{x}^2 + \bar{y}^2 + \mu_{01} + \mu_{10} = \text{const} \quad . \tag{6.36}$$

Applying (6.36) to the steady state we have

$$\bar{y}_s^2 + \mu_{10,s} = \bar{x}_o^2 + \bar{y}_o^2 + \mu_{01,0} + \mu_{10,0} \tag{6.37}$$

The numerical integrations were carried out with initial values satisfying the condition $\bar{x}_c^2 + \bar{y}_c^2 = 1$ and with $\mu_{01,0} = \mu_{10,0} = 0.1$, i.e. $\sigma_{01,0} = \sigma_{10,0} = 0.3162$. Under these conditions we find that the right hand side of (6.37) is 1.2. If another conservative quantity could be found we could determine the steady state completely. However, since it has been impossible to do so, we shall use the numerical integrations and (6.37) becomes then a check on the accuracy of the numerical scheme. From this series of experiments it was found that the Runge-Kutta method is very accurate in satisfying (6.37). In addition, the numerical experiments showed that in the asymptotic state we have $\bar{x}(\infty) = \mu_{10}(\infty) = \mu_{11}(\infty) = 0$, while $\mu_{01}(\infty) = \mu_{01}(0)$. Using this experimental value we find from (6.37) that $y_s^2 = 1.1$ and $y_s = -1.0488$. This value was reproduced with excellent accuracy in the numerical experiments. The solution based on the closure assumption must then be compared with the exact value which for the adopted value of $\mu_{01}(0) = \mu_{10}(0) = 0.1$ is $\bar{y}(\infty) = -1.0516$. The difference between the values based on the exact and the closure calculations is thus in this case about 0.25%. Repeating the numerical integrations for a number of values of $\mu_{10}(0) = \mu_{01}(0)$ it turns out that $\mu_{01}(\infty) = \mu_{01}(0)$.

Using this experimental fact we may use (6.37) to calculate $\bar{y}_s = \bar{y}(\infty)$. Under the experimental condition we have $\bar{x}^2 + \bar{y}^2 = 1$, $\mu_{01}(0) = \mu_{10}(0) = \sigma_o^2$ and $\mu_{10,s} = \mu_{10}(\infty) = \mu_{10}(0)$. Consequently,

$$\bar{y}(\infty) = -(1 + \sigma_o^2)^{\frac{1}{2}} \qquad (6.38)$$

Values of $\bar{y}(\infty) = \bar{y}_c(\infty)$, computed from (6.38), are listed in the following table as a function of σ_o together with the values of $\bar{y}(\infty)$ reproduced from the previous table.

Table 3

showing values of $\bar{y}_c(\infty)$ computed from (6.38) as a function of σ_o together with values of $\bar{y}(\infty)$ from the exact solution. Assumptions: $\bar{x}_o^2 + \bar{y}_o^2 = 1$, $\mu_{01}(0) = \mu_{10}(0) = \sigma_o^2$ and $\mu_{10}(\infty) = \mu_{10}(0)$.

σ_o	$\bar{y}(\infty)$	$\bar{y}_c(\infty)$
1.0000	- 1.55	- 1.41
0.7071	- 1.28	- 1.22
0.5000	- 1.14	- 1.12
0.4082	- 1.09	- 1.08
0.3536	- 1.07	- 1.06
0.3162	- 1.05	- 1.05
0.2500	- 1.03	- 1.03
0.2236	- 1.02	- 1.02

It is seen that $\bar{y}_c(\infty)$ deviates little from the exact $\bar{y}(\infty)$ whenever σ_o is small but quite large differerences are found for large values of σ_o. The closure assumption is thus justified for small uncertainties as also indicated by the fact that the exact values of $\mu_{10}(\infty)$ approach $\mu_{10}(0)$ for small values of σ_o.

Some examples of trajectories, computed on the basis of the system (6.16) are shown in Figure 11a, b, and c. The first of these, Fig. 11a, started from the position $(\bar{x}_o, \bar{y}_o) = (1,0)$ with $\mu_{10}(0) = \mu_{01}(0) = 0.1$, i.e. $\sigma_{10}(0) = \sigma_{01}(0) = 0.3$. The position is shown in Figure 11a in the upper right hand corner surrounded by an initial uncertainty circle. For each point on the trajectory the uncertainty ellipse (see Appendix 2) has been drawn.

As the trajectory approaches the asymptotic state, the uncertainty ellipse becomes gradually smaller until it collapses into a line ($\mu_{10}(\infty) = \mu_{11}(\infty) = 0$) parallel to the y - axis. Figure 11b shows the trajectory and the uncertainty ellipses for the initial conditions $(\bar{x}_o, \bar{y}_o) = (0.6, 0.8)$, $\mu_{01}(0) = \mu_{10}(0) = 0.1$, while Figure 11c depicts the situation for the initial conditions $(\bar{x}_o, \bar{y}_o) = (0.1, 0.995)$, $\mu_{01}(0) = \mu_{10}(0) = 0.1$. In all cases, but especially the last one, it is seen that the trajectories deviate very much from the deterministic trajectory which in all cases is the unit circle. The shape of the trajectory in Figure 11c can be explained qualitatively from the fact that many of the points within the initial uncertainty circle are in the half plane $\bar{x} < 0$. These points will, in a deterministic sense, have trajectories which are circles in $\bar{x} < 0$, but all with an asymptotic state on the negative part of the y - axis.

Although no solutions to the system (6.16) in a closed form have been found, we may find some properties which can help to explain the experimental behaviour shown in Figure 11a, b, and c. Consider for example the area of the uncertainty ellipse. Using the formulas given in Appendix 2, we find after some evaluations that the area A_E is

$$A_E = 8\pi l(\mu_{01}\mu_{10} - \mu_{11}^2)^{\frac{1}{2}} \tag{6.39}$$

Using the last three equations in the system (6.16) we can obtain the result that

$$\frac{dA_E}{} = \tfrac{1}{2}\bar{y}.A_E \tag{6.40}$$

Since A_E by definition is positive it follows from (6.40) that the area of the uncertainty ellipse increases as long as $\bar{y} > 0$, but will start to decrease when $\bar{y}$ becomes negative as it will because we know that $\bar{y}(\infty)$ is negative.

Figure 12 shows a comparison of trajectories computed in two different ways. Both trajectories start from the same point (0.7, 0.7) with the same uncertainty ($\mu_{01} = \mu_{10} = 0.8$) but one of them (marked by circles) is obtained from the closure scheme, i.e. numerical integration of the system (6.16), while the other (marked by crosses) we obtained by an evaluation of the integrals (6.6). The closure scheme gives accurate results for small times, but the two trajectories differ significantly when they approach the asymptotic states.

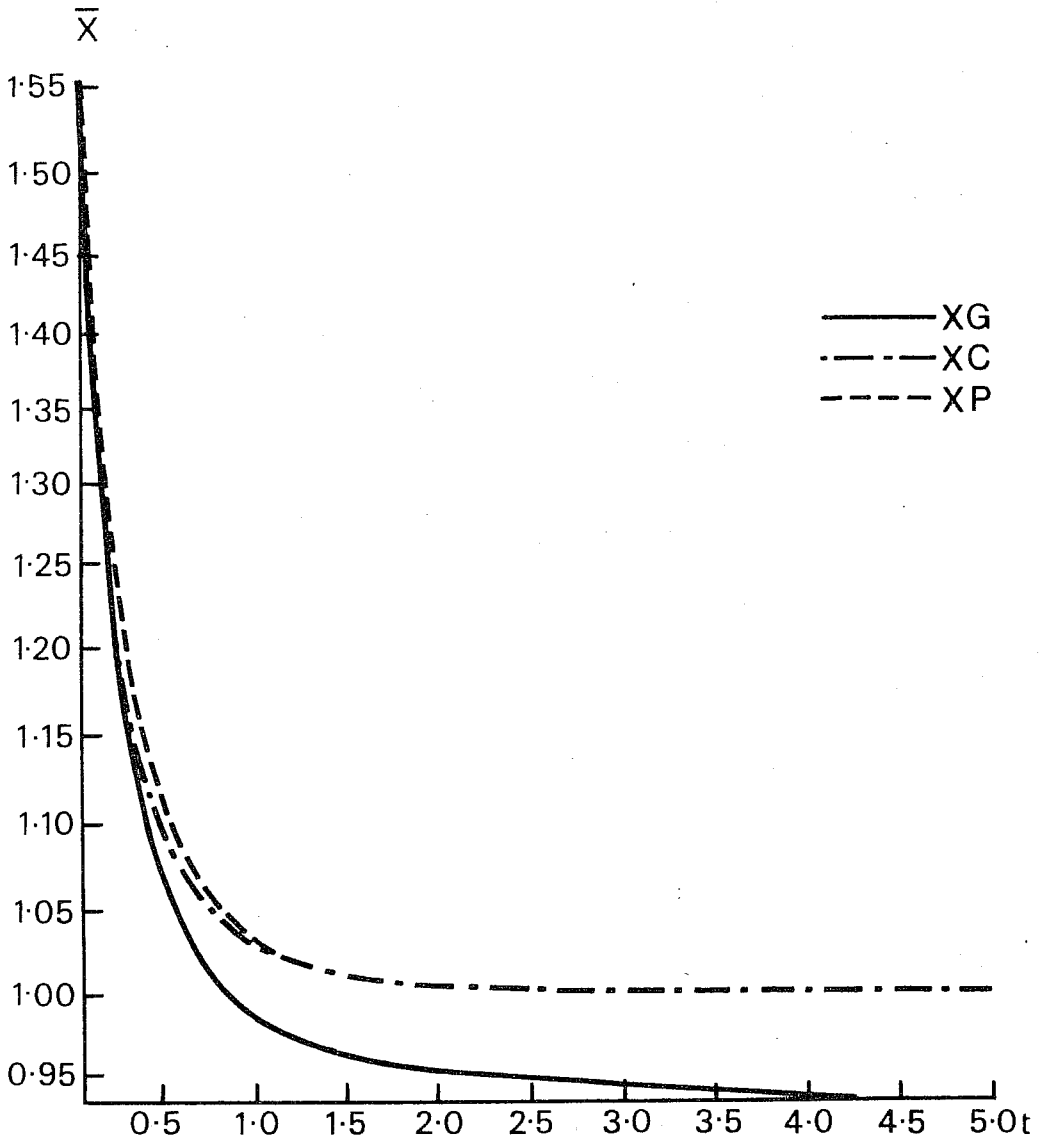

Fig. 6a : $\bar{x} = \bar{x}(t)$ with initial conditions $x_0 = 2$, $\sigma_0 = 1$, corresponding to $p = 4$, $\beta = 0.5$, computed in three different ways. The full curve is obtained from the Gaussian probability function, the dashed curve from the Pearson probability function and the dashed-dotted curve from the closure scheme.

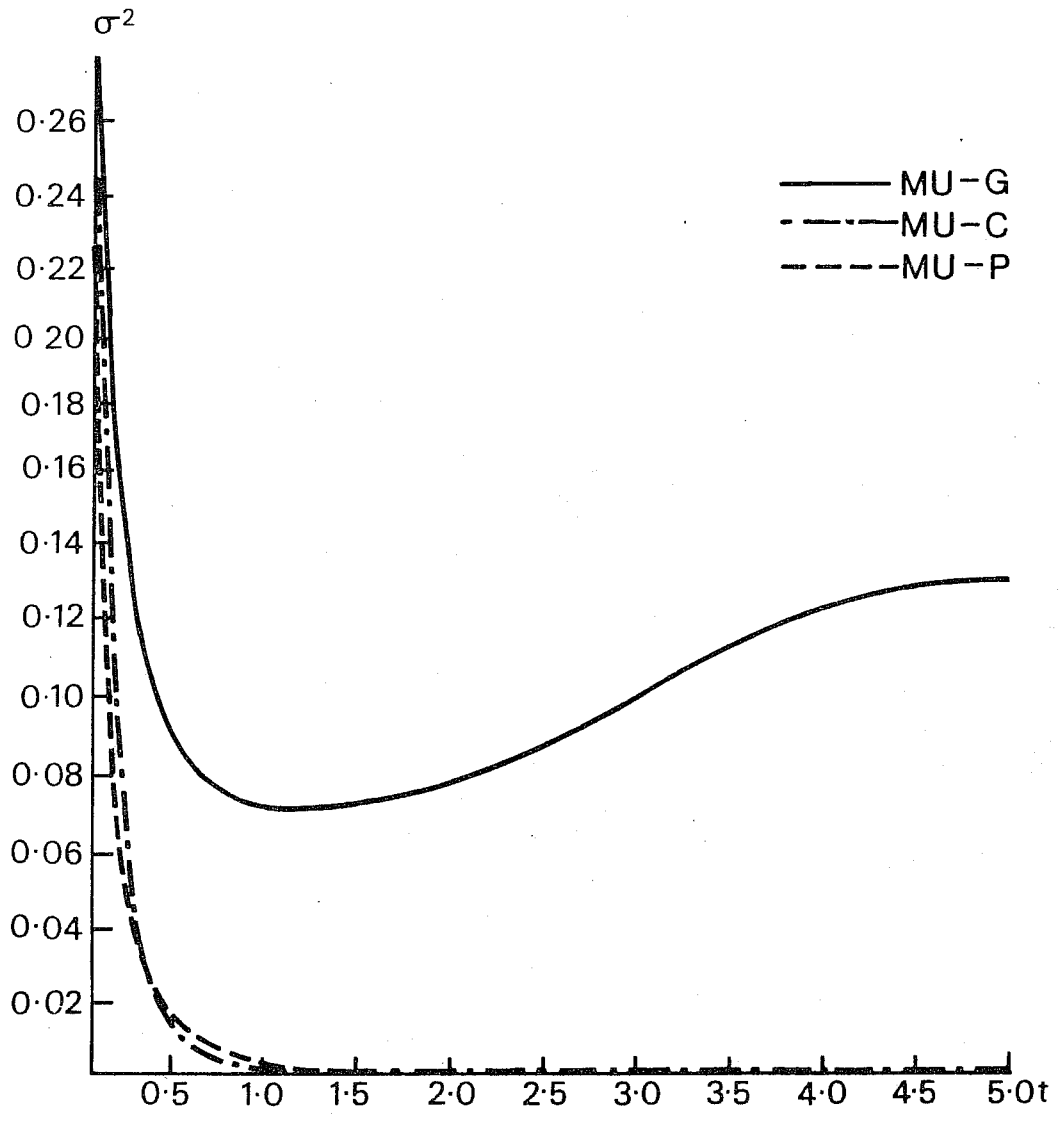

Fig. 6b : $\mu = \mu(t)$ with initial conditions $\bar{x}_o = 2$, $\sigma_o = 1$, computed in three different ways, Arrangement as in Fig. 6a.

7. Concluding remarks

The main purpose of the present paper is to illustrate the behaviour of some simple stochastic-dynamic systems at large times. At the same time, it has been possible to compare some exact solutions with solutions based upon a closure assumption.

It is found from the examples that the asymptotic behaviour of a given system depends on whether or not the deterministic system has one or more asymptotic steady states and on the nature of the probability density function. In addition, it is seen from the examples that large deviations between the deterministic and stochastic-dynamic solutions are found when the uncertainty in the initial state is non-negligible in some sense as compared to the mean value.

The only closure scheme applied here is the neglect of third and higher moments. From the examples, it is found that the closure scheme may introduce steady states not present in the exact stochastic-dynamic treatment. In the neighborhood of such a false steady state, created by the closure assumption, the solutions from the exact and approximate procedures are very different. Apart from these cases, there is good agreement between the exact and the closure solutions provided the initial uncertainty is small. If this is

not so, the closure solution becomes inaccurate presumably because the closure assumption is violated.

In our examples it is also seen that the asymptotic values of the uncertainty are on occasion either zero or less than the initial uncertainty. Such a result is obtained in the examples when the trajectory of the stochastic-dynamic system deviates from the trajectory of the deterministic system. We refer in this respect particularly to Section 6 where the behaviour is governed by the fact that the sum of the certain and uncertain energies has to remain constant.

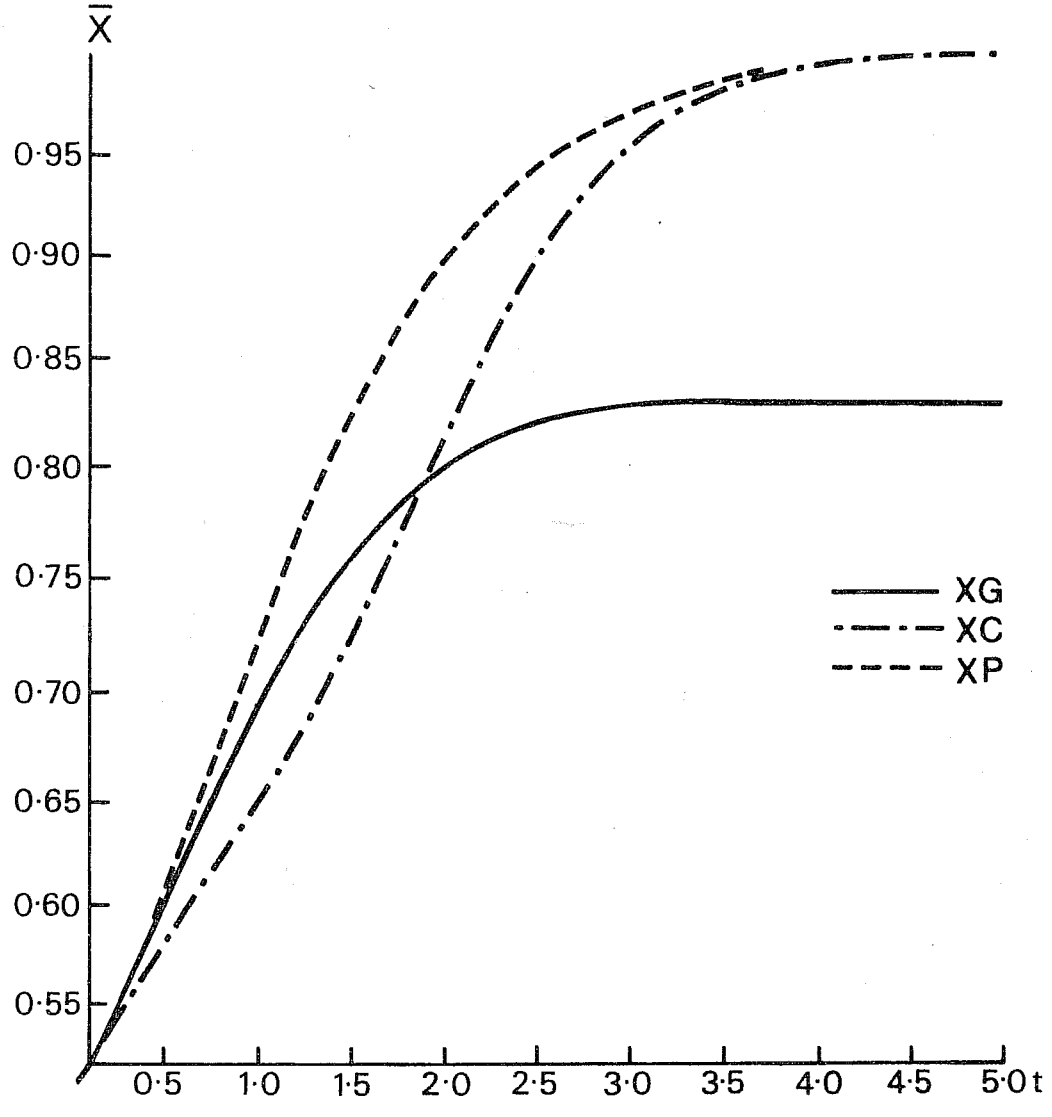

Fig. 7a : $\bar{x} = \bar{x}(t)$ with initial conditions $\bar{x}_0 = 0.5$, $\sigma_0 = 0.3535$, corresponding to $p = 2$, $\beta = 0.25$, computed in three different ways. Arrangement as in Fig. 6a.

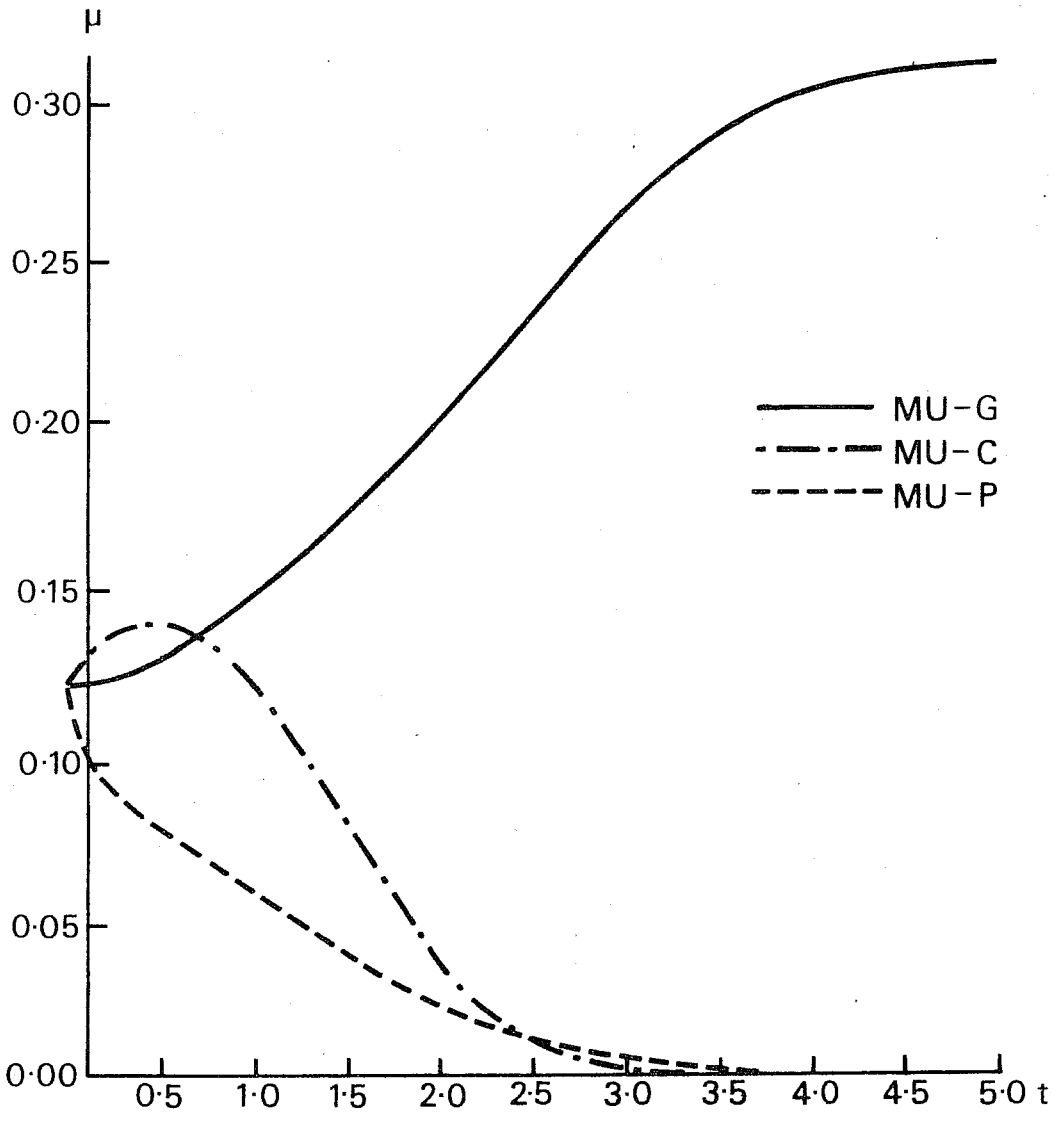

Fig. 7b : $\mu = \mu(t)$ with initial conditions $\bar{x}_c = 0.5$, $\sigma_c = 0.3535$, corresponding to $p = 2$ and $\beta = 0.25$, computed in three different ways. Arrangement as in Fig. 6a.

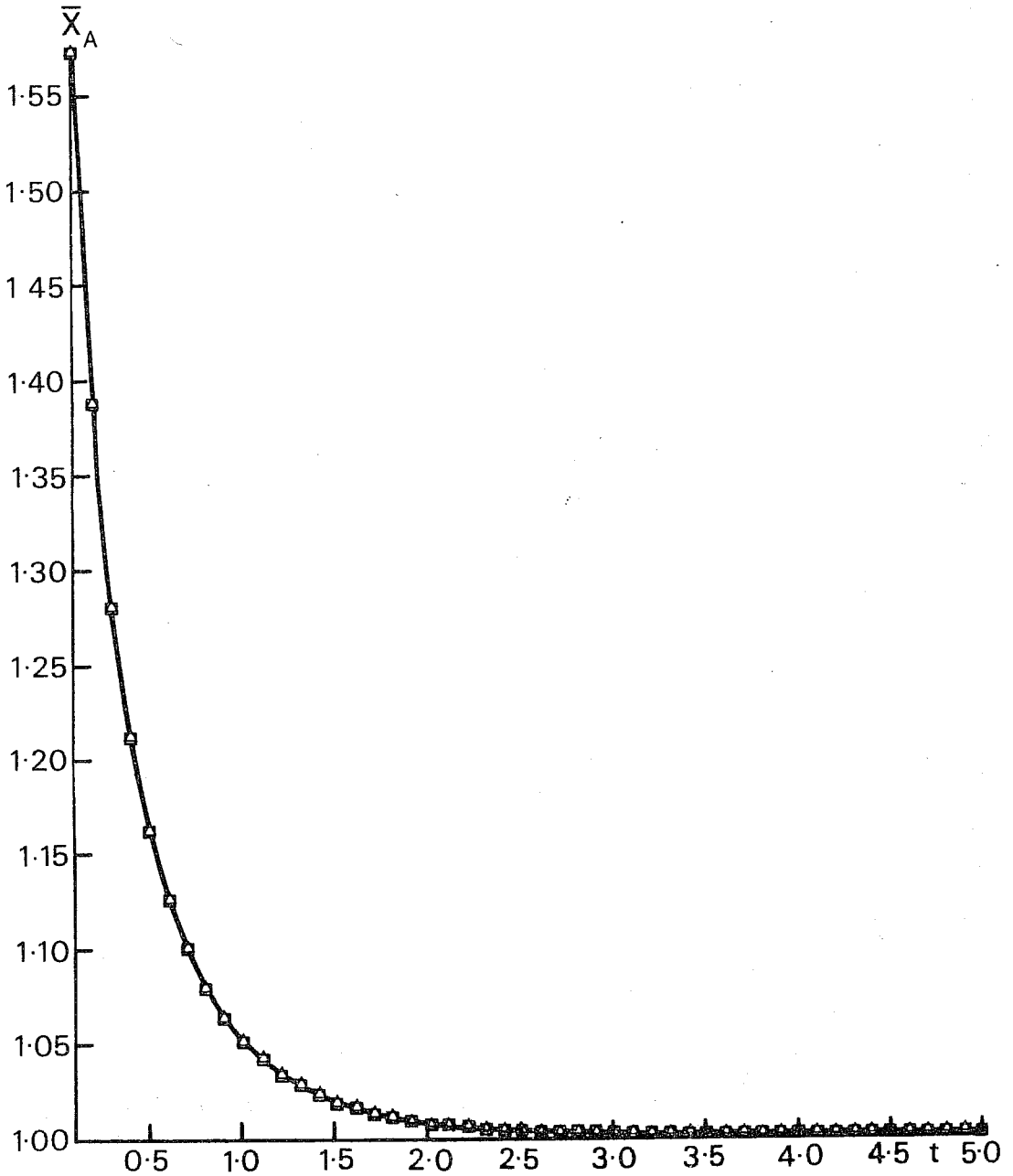

Fig. 8a : $\bar{x} = \bar{x}(t)$ computed by a Monte Carlo procedure with initial conditions $\bar{x}_o = 2$, $\sigma = 0.5$. Squares and triangles indicate points computed from samples of 5 and 21 points respectively.

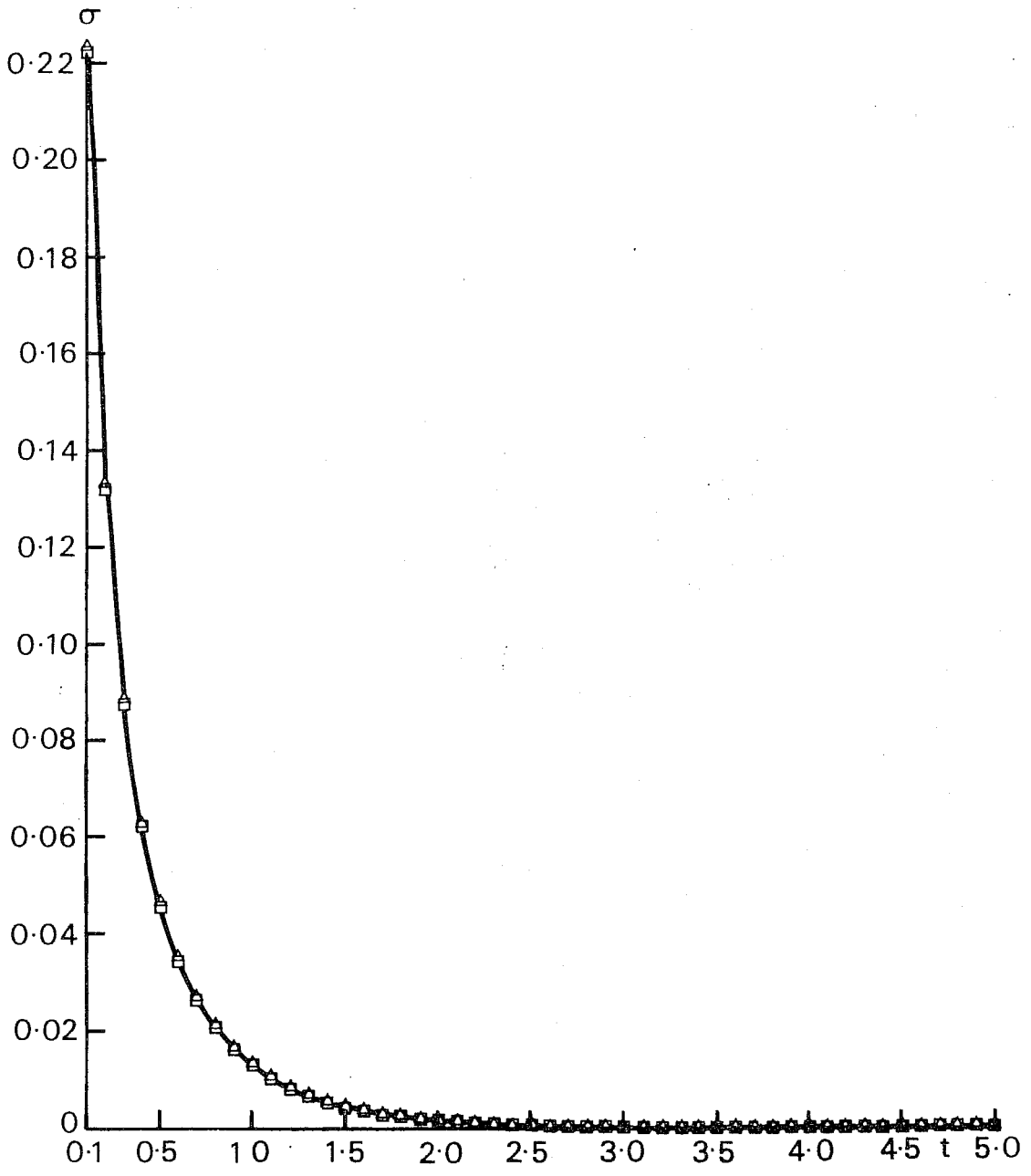

Fig. 8b : $\sigma = \sigma(t)$ for the case described in Fig. 8a.

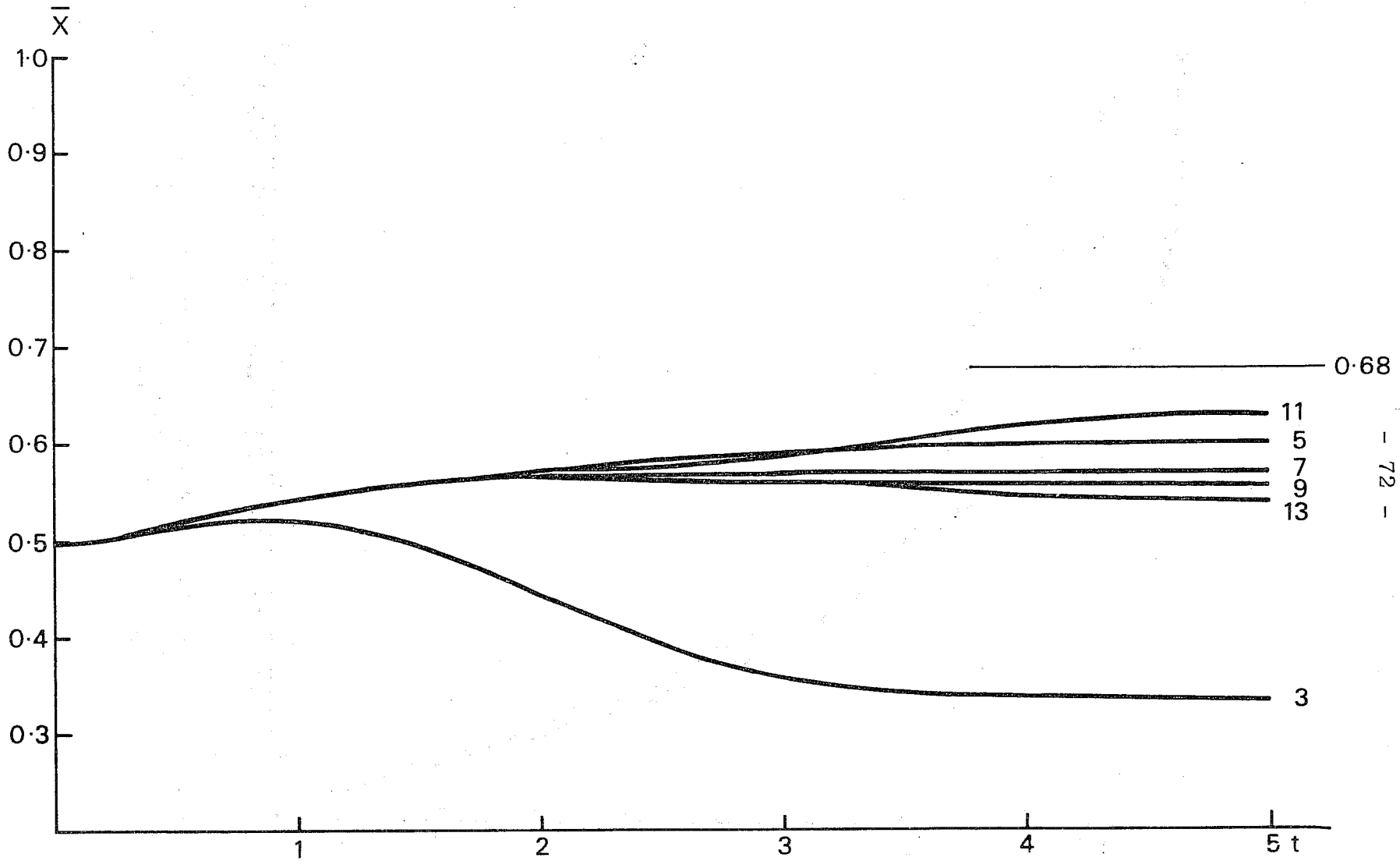

Fig. 9 : $\bar{x} = \bar{x}(t)$ computed by a Monte Carlo procedure with initial conditions $\bar{x}_0 = 0.5$, $\sigma_0 = 0.5$. The curves are obtained from samples with the number of elements marked on each curve. The theoretical value is indicated by the line marked 0.68.

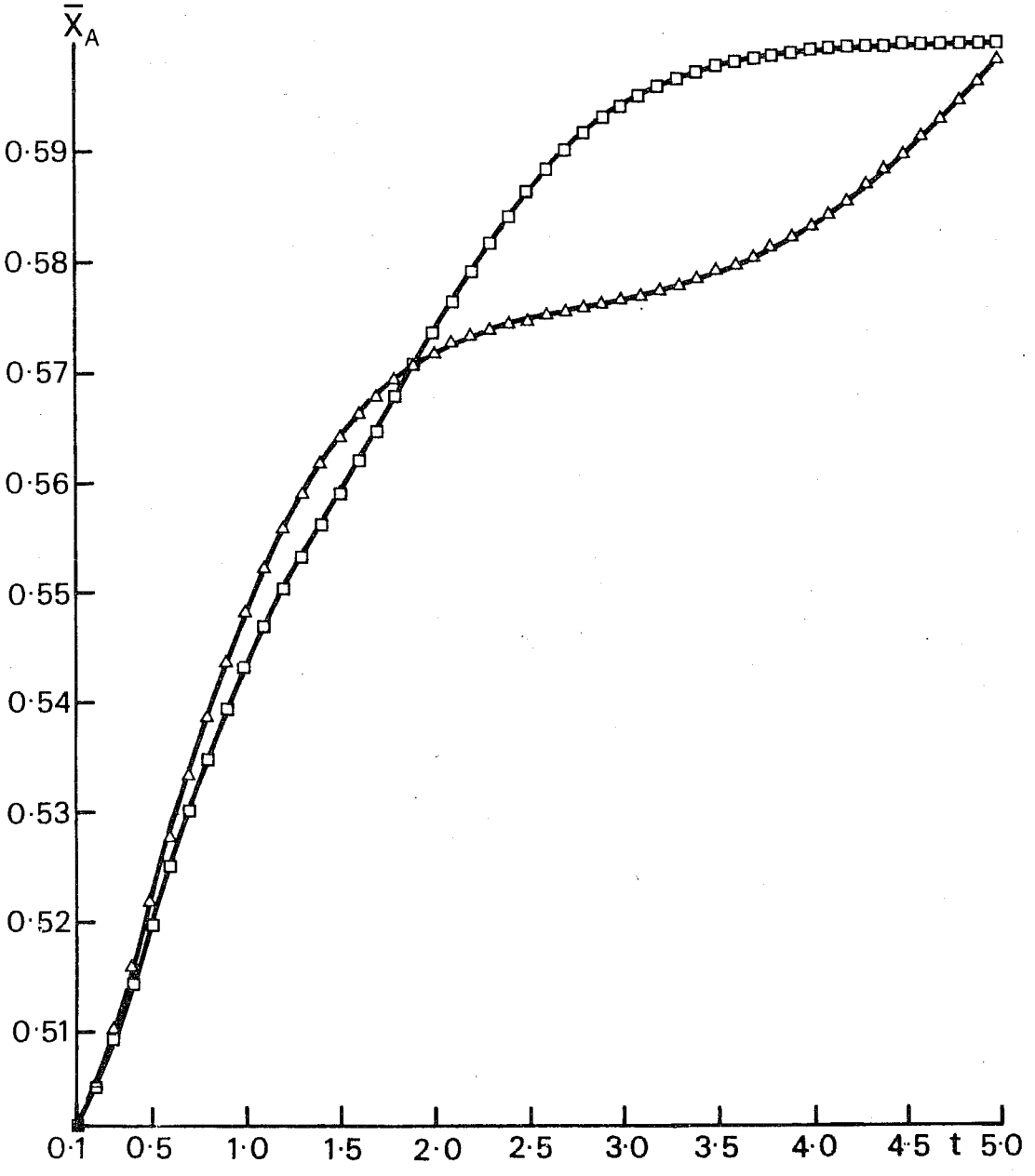

Fig. 10a : $\dot{x} = \dot{x}(t)$ computed by a Monte Carlo procedure with initial conditions $\dot{x}_o = 0.5$, $\sigma_o = 0.5$. Arrangement as in Fig. 8a.

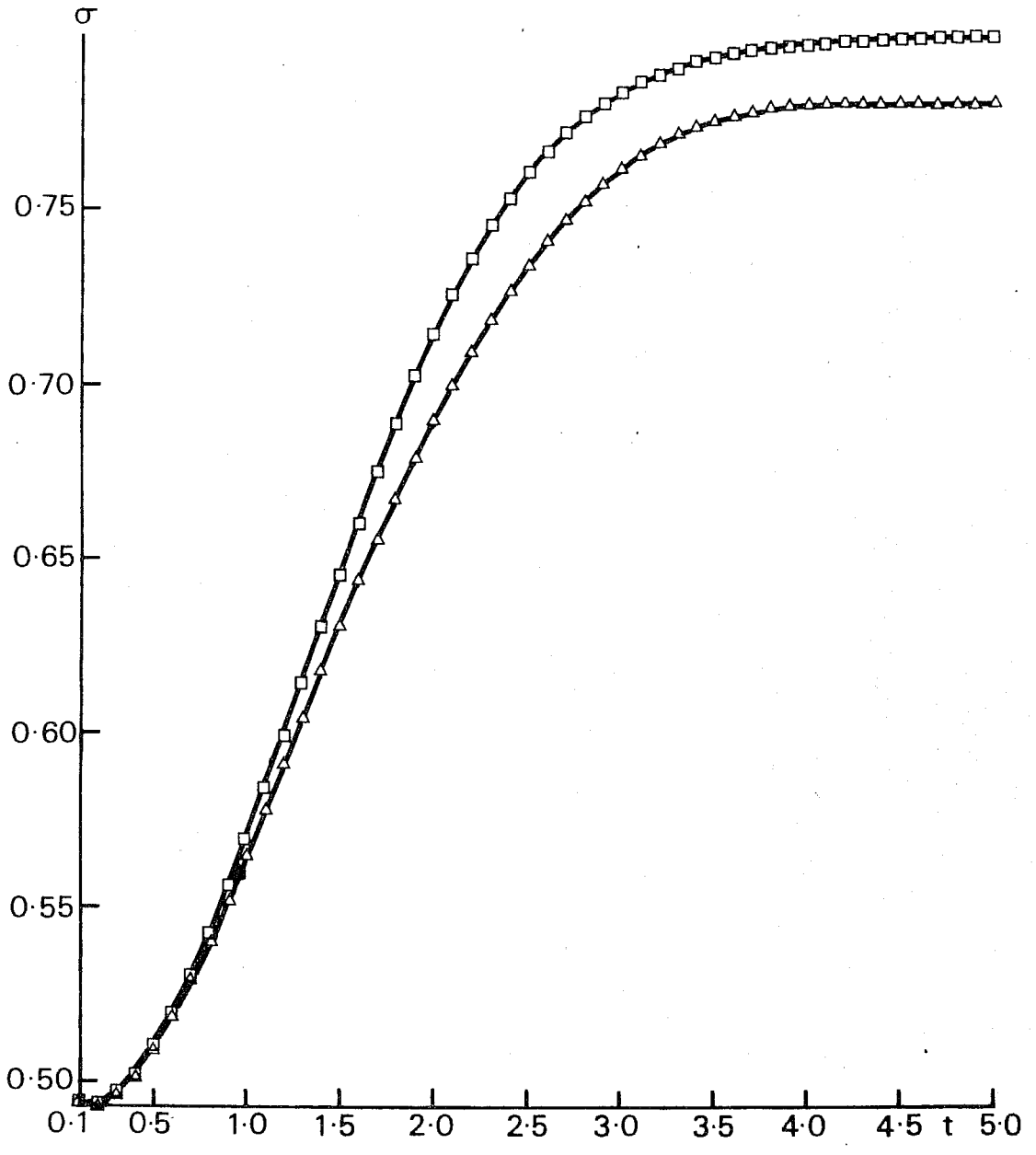

Fig. 10b : $\sigma = \sigma(t)$ for the case described in Fig. 10a.

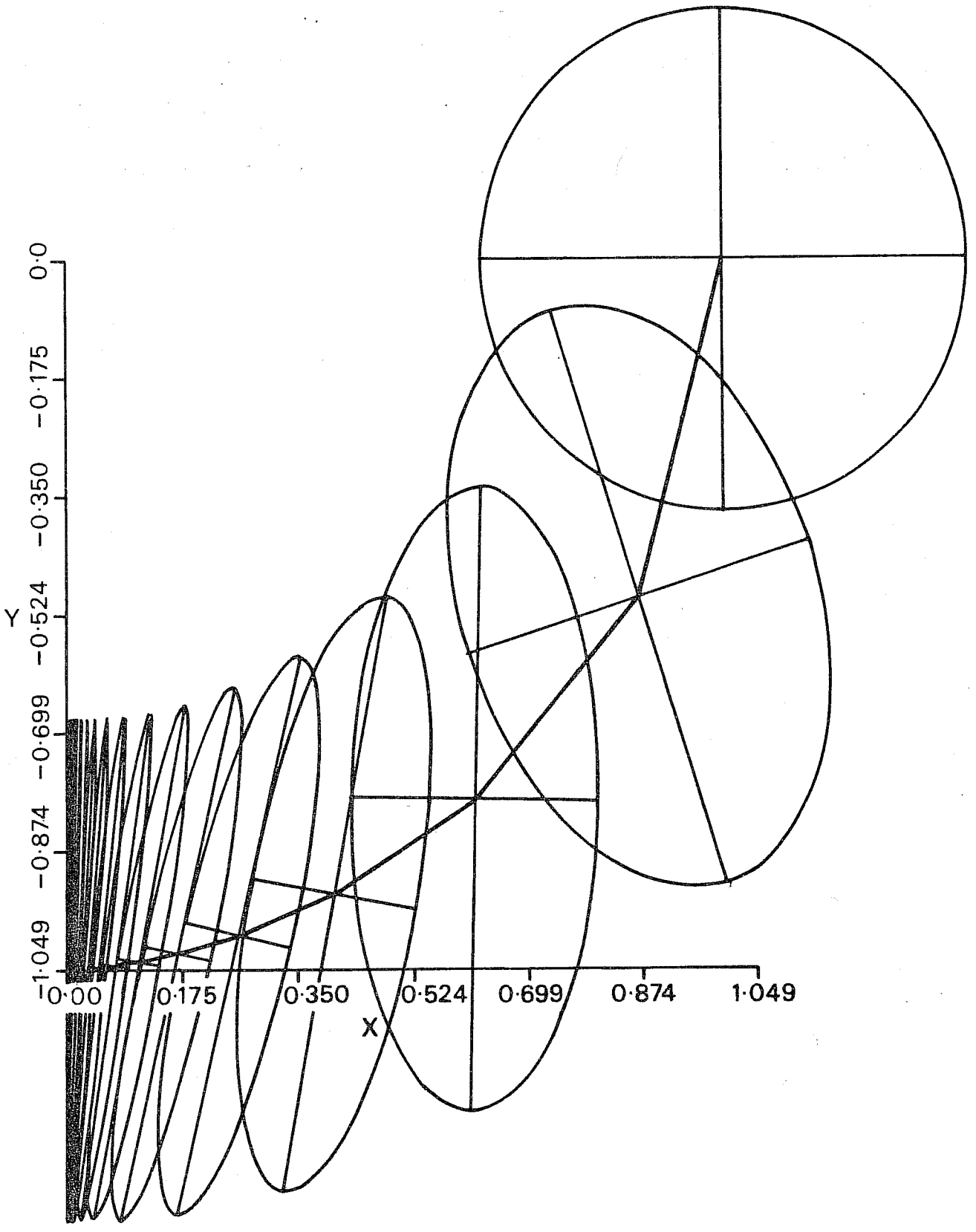

Fig. 11a : $\bar{x} = x(t)$, $\bar{y} = y(t)$ based on a numerical integration of the system (6.16) from initial conditions $\bar{x}_0 = 1$, $\bar{y}_0 = 0$, $\mu_{10}(0) = \mu_{01}(0) = 0.1$, $\mu_{11}(0) = 0$. The uncertainty ellipses are constructed according to Appendix 2.

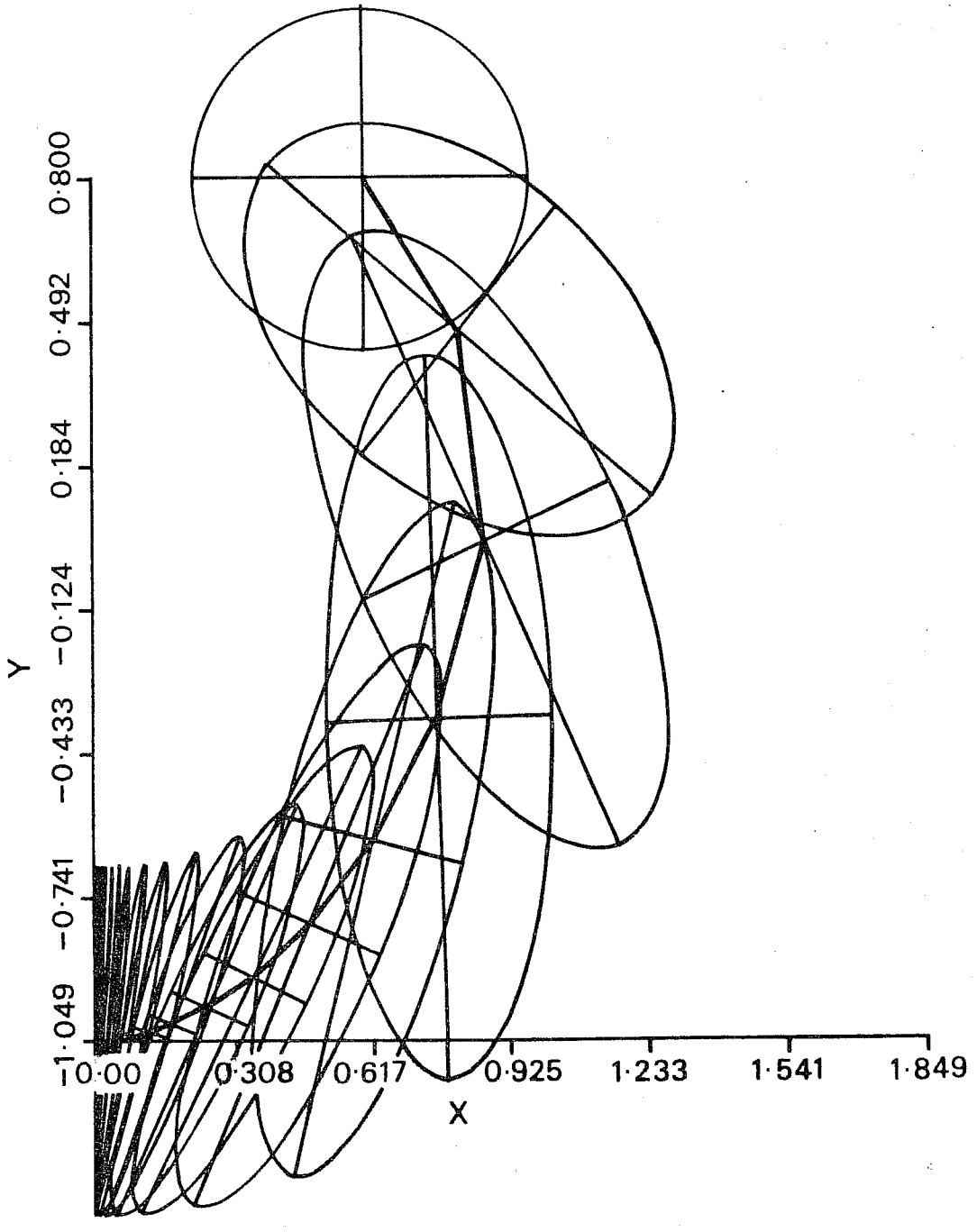

Fig. 11b : Initial conditions $\bar{x}_0 = 0.6$, $\bar{y}_0 = 0.8$, $\mu_{10}(0) = \mu_{01}(0) = 0.1$, $\mu_{11}(0) = 0$.
Arrangement as in Fig. 11a.

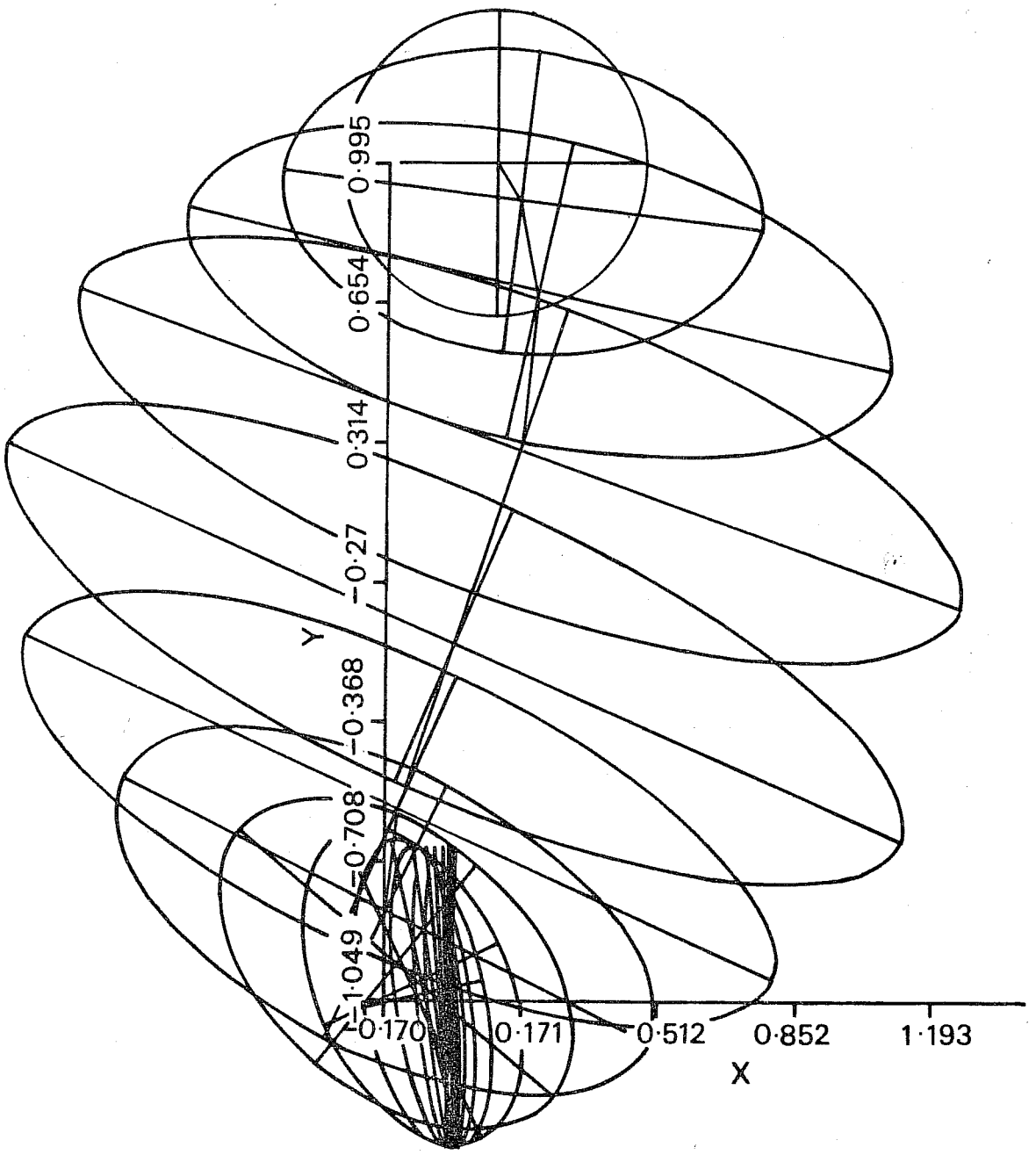

Fig. 11c : Initial conditions $\bar{x}_0 = 0.1$, $\bar{y}_0 = 0.995$, $\mu_{01} = \mu_{10}(0) = 0.1$, $\mu_{11}(0) = 0$. Arrangement as in Fig. 11a.

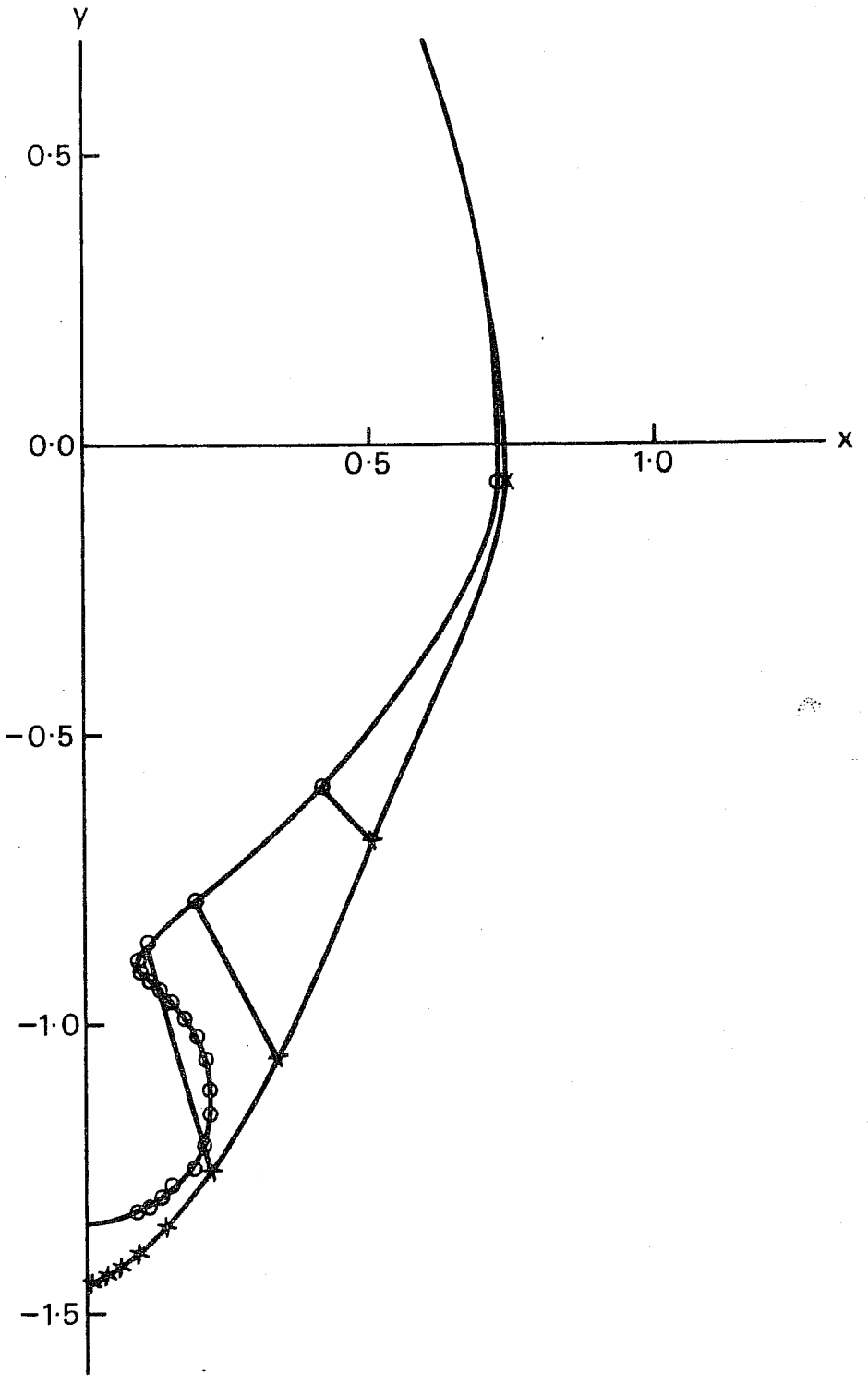

Fig. 12 : $\bar{x}(t)$, $\bar{y}(t)$ with initial conditions $\dot{x}_0 = \dot{y}_0 = 0.7$, $\mu_{01}(0) = \mu_{10}(0) = 0.8$, $\mu_{11}(0) = 0$ computed from the exact solution (crosses) and the closure approximation (circles). Connecting lines give positions at the same time.

References

Abramowitz M. and I. Stegun, 1965: Handbook of Mathematical Functions, Dover Publications, New York, 1046 pp.

Epstein, E. S., 1969: Stochastic dynamic predictions, Tellus, Vol. 21, pp. 739-759.

Fleming, R. J.,1971a: On stochastic dynamic prediction: I The energetics of uncertainty and the question of closure, Monthly Weather Review, Vol. 99, pp. 851-872.

Fleming, R. J., 1971b: On stochastic dynamic prediction: II Predictability and utility, Monthly Weather Review, Vol. 99, pp. 927-938.

Gradshteyn, I. S. and I. M. Ryzhik, 1965: Table of Integrals, Series and Products, Academic Press, New York and London, 1086 pp.

Leith, C. E., 1975: Statistical and Statistical-Dynamical Methods in Medium-Range Weather Forecasts, Proceedings of Seminars on the Scientific Foundation of Medium-Range Weather Forecasts, pp. 307-379.

May, R., 1976: Theoretical Ecology.

Pitcher, E. J. 1974: Stochastic dynamic prediction using atmospheric data, Ph.D. Dissertation, University of Michigan (Available through Library of Congress).

Wiin-Nielsen, A., 1975: Predictability and climate variation illustrated by a low-order system, Proceedings of Seminars on Scientific Foundation of Medium-Range Weather Forecasts, pp. 258-306.

Captions

Fig. 1a : $\bar{x} = \bar{x}(t)$ with initial conditions $\bar{x}_0 = 0.5$ and $\sigma_0 = 0.5$ obtained from the closure solution (3.13) and (3.14).

Fig. 1b : $\sigma = \sigma(t)$ with initial conditions $\bar{x}_0 = 0.5$ and $\sigma_0 = 0.5$ obtained from the closure solution (3.13) and (3.14).

Fig. 1c : The third moment $\mu_3 = \mu_3(t)$ with the initial conditions $\bar{x}_0 = 0.5$ and $\sigma_0 = 0.5$ calculated from (2.29) and (2.30).

Fig. 2a : $\bar{x} = \bar{x}(t)$ with initial conditions $\bar{x}_0 = 0.3$ and $\sigma_0 = 0.1732$, corresponding to $p = 3$ and $\beta = 0.1$, calculated from (2.15). The small circles are points $\bar{x} = \bar{x}(t)$ calculated from the closure solution (3.13) and (3.14).

Fig. 2b : $\sigma = \sigma(t)$ with initial conditions $\bar{x}_0 = 0.3$ and $\sigma_0 = 0.1732$, calculated from (2.24) and (2.25). The curve with the small circles is $\sigma = \sigma(t)$ with the same initial conditions computed from (3.13) and (3.14).

Fig. 2c : The third moment $\mu_3 = \mu_3(t)$ with the initial conditions $\bar{x}_0 = 0.3$ and $\sigma_0 = 0.1732$ calculated from (2.29) and (2.30).

Fig. 3a : Initial conditions are $\bar{x}_0 = 19^{\frac{1}{2}}$, $\sigma_0 = 1$, corresponding to $p = 19$, $\beta = 19^{-\frac{1}{2}}$. Arrangement as in Fig. 2a.

Fig. 3b : Initial conditions $\bar{x}_0 = 19^{\frac{1}{2}}$, $\sigma_0 = 1$, corresponding to $p = 19$, $\beta = 19^{-\frac{1}{2}}$. Arrangement as in Fig. 2b.

Fig. 3c : Initial conditions $\bar{x}_0 = 19^{\frac{1}{2}}$, $\sigma_0 = 1$, corresponding to $p = 19$, $\beta = 19^{-\frac{1}{2}}$. Arrangement as in Fig. 2c.

Fig. 4 : $\bar{x} = \bar{x}(t)$ computed from (3.24) with $\bar{x}_0 = 1.1$, $\sigma_0 = 0.5$.

Fig. 5a : $\bar{x} = \bar{x}(t)$ computed from (4.28) and (4.30) by numerical integration with initial conditions $\bar{x}_0 = 0.5$, $\sigma_0 = 0.5$, i.e. $\mu_0 = 0.25$.

Fig. 5b : $\mu = \mu(t)$ computed from (4.28) and (4.30) by numerical integration with initial conditions $\bar{x}_0 = 0.5$, $\mu_0 = 0.25$.

Fig. 6a : $\bar{x} = \bar{x}(t)$ with initial conditions $\bar{x}_0 = 2$, $\sigma_0 = 1$, corresponding to $p = 4$, $\beta = 0.5$, computed in three different ways. The full curve is obtained from the Gaussian probability function, the dashed curve from the Pearson probability function and the dashed-dotted curve from the closure scheme.

Fig. 6b : $\mu = \mu(t)$ with initial conditions $\bar{x}_o = 2$, $\sigma_o = 1$, computed in three different ways. Arrangement as in Fig. 6a.

Fig. 7a : $\bar{x} = \bar{x}(t)$ with initial conditions $\bar{x}_o = 0.5$, $\sigma_o = 0.3535$, corresponding to $p = 2$, $\beta = 0.25$, computed in three different ways. Arrangement as in Fig. 6a.

Fig. 7b : $\mu = \mu(t)$ with initial conditions $\bar{x}_o = 0.5$, $\sigma_o = 0.3535$, corresponding to $p = 2$ and $\beta = 0.25$, computed in three different ways. Arrangement as in Fig. 6a.

Fig. 8a : $\bar{x} = \bar{x}(t)$ computed by a Monte Carlo procedure with initial conditions $\bar{x}_o = 2$, $\sigma_o = 0.5$. Squares and triangles indicate points computed from samples of 5 and 21 points respectively.

Fig. 8b : $\sigma = \sigma(t)$ for the case described in Fig. 8a.

Fig. 9 : $\bar{x} = \bar{x}(t)$ computed by a Monte Carlo procedure with initial conditions $\bar{x}_o = 0.5$, $\sigma_o = 0.5$. The curves are obtained from samples with the number of elements marked on each curve. The theoretical value is indicated by the line marked 0.68.

Fig.10a : $\bar{x} = \bar{x}(t)$ computed by a Monte Carlo procedure with initial conditions $\bar{x}_o = 0.5$, $\sigma_o = 0.5$. Arrangement as in Fig. 8a.

Fig.10b : $\sigma = \sigma(t)$ for the case described in Fig. 10a.

Fig.11a : $\bar{x} = \bar{x}(t)$, $\bar{y} = \bar{y}(t)$ based on a numerical integration of the system (6.16) from initial conditions $\bar{x}_0 = 1$, $\bar{y}_0 = 0$, $\mu_{10}(0) = \mu_{01}(0) = 0.1$, $\mu_{11}(0) = 0$. The uncertainty ellipses are constructed according to Appendix 2.

Fig.11b : Initial conditions $\bar{x}_0 = 0.6$, $\bar{y}_0 = 0.8$, $\mu_{10}(0) = \mu_{01}(0) = 0.1$, $\mu_{11}(0) = 0$. Arrangement as in Fig. 11a.

Fig.11c : Initial conditions $\bar{x}_0 = 0.1$, $\bar{y}_0 = 0.995$, $\mu_{01} = \mu_{10}(0) = 0.1$, $\mu_{11}(0) = 0$. Arrangement as in Fig. 11a.

Fig.12 : $\bar{x}(t)$, $\bar{y}(t)$ with initial conditions $\bar{x}_0 = \bar{y}_0 = 0.7$, $\mu_{01}(0) = \mu_{10}(0) = 0.8$, $\mu_{11}(0) = 0$ computed from the exact solution (crosses) and the closure approximation (circles). Connecting lines give positions at the same time.

Appendix 1

We consider the integral

$$J = \int_{-\infty}^{+\infty} \frac{1}{z} e^{-(z-n)^2} dz \,. \qquad (A.1)$$

To evaluate (A.1) we write it in the following way

$$J = \lim_{\varepsilon \to 0} \left\{ \int_{-\infty}^{-\varepsilon} z^{-1} e^{-(z-n)^2} dz + \int_{\varepsilon}^{\infty} z^{-1} e^{-(z-n)^2} dz \right\} . \qquad (A.2)$$

Replacing z by (-z) in the first integral we find

$$J = \lim_{\varepsilon \to 0} \int_{\varepsilon}^{\infty} z^{-1} \left(e^{-(z-n)^2} - e^{-(z+n)^2} \right) dz \qquad (A.3)$$

or,

$$J = e^{-n^2} \lim_{\varepsilon \to 0} \int_{\varepsilon}^{\infty} z^{-1} . e^{-z^2} . \left(e^{2nz} - e^{-2nz} \right) dz \,. \qquad (A.4)$$

Using the series expansion for the exponential functions, we may write (A.4) in the form

$$J = e^{-n^2} \int_{0}^{\infty} e^{-z^2} . 2 . \sum_{r=0}^{\infty} \frac{(2n)^{2r+1}}{(2r+1)\,!} z^{2r} dz \,. \qquad (A.5)$$

Writing $u = z^2$ we get

$$J = e^{-n^2} \int_0^{\infty} e^{-u} \sum_{r=0}^{\infty} \frac{(2n)^{2r+1}}{(2r+1)\,!}\; u^{r-\frac{1}{2}}\; du\,, \qquad (A.6)$$

which may be integrated term by term giving:

$$J = e^{-n^2} \sum_{r=0}^{\infty} \frac{(2n)^{2r+1}}{(2r+1)\,!}\; (r-\tfrac{1}{2})\,! = (-\tfrac{1}{2})\,!\; e^{-n^2} \sum_{r=0}^{\infty} \frac{(2n)^{2r+1}}{(2r+1)\,!}\; \frac{(2r-1)\,!}{2^{2r-1}(r-1)\,!}$$

$$(A.7)$$

where we have made use of the identity:

$$(r-\tfrac{1}{2})\,! = (r-\tfrac{1}{2})(r-\frac{3}{2})..(\tfrac{1}{2})(-\tfrac{1}{2})\,! = (-\tfrac{1}{2})\,!\; \frac{(2r-1)\,!}{2^{2r-1}(r-1)\,!}$$

$$(A.8)$$

Rearranging (A.7) we get:

$$J = 2(-\tfrac{1}{2})\,!\; e^{-n^2} \sum_{r=0}^{\infty} \frac{1}{r\,!}\; \frac{n^{2r+1}}{(2r+1)} \qquad (A.9)$$

We note that

$$\int_0^n s^{2r}\; ds = \frac{n^{2r+1}}{2r+1} \qquad (A.10)$$

Substituting (A.10) in (A.9) we find

$$J = 2\sqrt{\pi}\, e^{-n^2} \int_0^n \left\{ \sum_{r=0}^{\infty} \frac{(s^2)^r}{r!} \right\} ds \qquad (A.11)$$

or,

$$J = 2\sqrt{\pi}\, e^{-n^2} \int_0^n e^{s^2}\, ds\,. \qquad (A.12)$$

(A.12) is identical to (2.21) which thus has been established.

Appendix 2

The uncertainty ellipse has been used by Fleming (1971) and is defined by the expression

$$\frac{x^2}{\mu_{10}} - 2\frac{r}{(\mu_{10}\cdot\mu_{01})^{\frac{1}{2}}}xy + \frac{y^2}{\mu_{01}} = 2(1-r^2)\ell \quad (A.13)$$

in which r is the correlation coefficient, i.e.

$$r = \frac{\mu_{11}}{(\mu_{10}\cdot\mu_{01})^{\frac{1}{2}}} \quad (A.14)$$

while ℓ is a constant chosen in such a way that $1 - \exp(-\ell)$ measures the probability that a point is inside the ellipse. ℓ is normally selected as $\ell = \ln.2$ in which case the probability is 0.5.

Using (A.14) we may write (A.13) in the form:

$$\frac{x^2}{\mu_{10}} - 2\frac{\mu_{11}}{\mu_{10}\mu_{01}}xy + \frac{y^2}{\mu_{01}} = 2\ell(1-r^2) \quad (A.15)$$

The equation (A.15) may be brought into the standard form by turning the coordinate system an angle θ. It turns out that θ is determined by the expressions

$$\cos 2\theta = \frac{\mu_{10}-\mu_{01}}{s}, \quad \sin 2\theta = \frac{2\mu_{11}}{s},$$

$$s = \left[(\mu_{01}-\mu_{10})^2 + 4\mu_{11}^2\right]^{\frac{1}{2}} \quad (A.16)$$

while (A.15) becomes

$$\frac{x_1^2}{\left(\frac{2\ell(1-r^2)}{A}\right)} + \frac{y_1^2}{\left(\frac{2\ell(1-r^2)}{B}\right)} = 1 , \qquad (A.17)$$

where

$$A = \frac{1}{2\mu_{01}\mu_{10}} \left((\mu_{01} + \mu_{10}) - s \right) , \qquad (A.18)$$

$$B = \frac{1}{2\mu_{01}\mu_{10}} \left((\mu_{01} + \mu_{10}) + s \right) . \qquad (A.19)$$

Appendix 3

Consider a sample with the mean $\bar{x}$ and the standard deviation σ. We have

$$\bar{x} = \frac{1}{N} \sum_{i=1}^{N} x_i \tag{A.20}$$

and

$$\sigma^2 = \frac{1}{N} \sum_{i=1}^{N} (x_i - \bar{x})^2 \tag{A.21}$$

We shall consider a simple procedure to construct a sample of points which has given values of $\bar{x}$ and σ. Let us select

$$\bar{x}-y_m, \quad \ldots, \quad \bar{x}-y_1, \quad \bar{x}, \quad \bar{x}+y_1, \quad \ldots, \quad \bar{x}+y_m. \tag{A.22}$$

It is obvious that the mean of this sample of $2m+1 = N$ points is $\bar{x}$. If we select a set of equidistant points which are d apart, we have $y_i = d.i$. Requiring that σ^2 shall have the prescribed value, we get

$$\frac{2}{2m+1} \cdot \sum_{j=1}^{m} y_i^2 = \frac{2}{2m+1} d^2 \sum_{j=1}^{m} j^2 = \frac{2d^2}{2m+1} \cdot \frac{1}{6} m(m+1)(2m+1), \tag{A.23}$$

or

$$\frac{1}{3} m(m+1)\, d^2 = \sigma^2 \tag{A.24}$$

giving

$$d = \sigma \left(\frac{3}{m(m+1)} \right)^{\frac{1}{2}}. \tag{A.25}$$

We note that the distance from the mean value to the largest value is

$$md = \sigma \left(3\frac{m}{m+1} \right)^{\frac{1}{2}} \qquad (A.26)$$

which for large values of m is $\sigma\sqrt{3}$.

Appendix 3

Consider a sample with the mean $\bar{x}$ and the standard deviation σ. We have

$$\bar{x} = \frac{1}{N} \sum_{i=1}^{N} x_i \tag{A.20}$$

and

$$\sigma^2 = \frac{1}{N} \sum_{i=1}^{N} (x_i - \bar{x})^2 \tag{A.21}$$

We shall consider a simple procedure to construct a sample of points which has given values of $\bar{x}$ and σ. Let us select

$$\bar{x}-y_m, \quad \ldots, \quad \bar{x}-y_1, \quad \bar{x}, \quad \bar{x}+y_1, \quad \ldots, \quad \bar{x}+y_m. \tag{A.22}$$

It is obvious that the mean of this sample of $2m+1 = N$ points is $\bar{x}$. If we select a set of equidistant points which are d apart, we have $y_i = d.i$. Requiring that σ^2 shall have the prescribed value, we get

$$\frac{2}{2m+1} \cdot \sum_{j=1}^{m} y_i^2 = \frac{2}{2m+1} d^2 \sum_{j=1}^{m} j^2 = \frac{2d^2}{2m+1} \cdot \frac{1}{6} m(m+1)(2m+1), \tag{A.23}$$

or

$$\frac{1}{3} m(m+1)\, d^2 = \sigma^2 \tag{A.24}$$

giving

$$d = \sigma \left(\frac{3}{m(m+1)} \right)^{\frac{1}{2}} . \tag{A.25}$$

We note that the distance from the mean value to the largest value is

$$md = \sigma \left(3\frac{m}{m+1} \right)^{\frac{1}{2}} \qquad (A.26)$$

which for large values of m is $\sigma\sqrt{3}$.

Appendix 4

Integrals involving $E_p(x)$.

The stochastic dynamic solutions presented in this paper require a knowledge of a number of integrals. In this appendix we collect a number of results which are not listed in the standard collections of integrals.

Consider first the integral

$$I_1 = \int_0^\infty \frac{z^p}{z+a} e^{-z} dz .$$

This integral may be calculated by considering the more general integral

$$I(m) = \int_0^\infty \frac{z^p}{z+a} e^{-m(z+a)} dz .$$

We note that for m = 1, we have

$$I(1) = e^{-a} I_1 \; ; \; I_1 = e^a I(1).$$

We find furthermore

$$\frac{dI}{dm} = -\int_0^\infty z^p e^{-m(z+a)} dz$$

$$\frac{dI}{dm} = - e^{-ma} \int_0^\infty z^p e^{-mz} dz$$

$$\frac{dI}{dm} = - e^{-ma} \frac{\Gamma(p+1)}{m^{p+1}} .$$

Noting furthermore that $I(\infty) = 0$, we find

$$I(m) = + \Gamma(p+1) \int_m^{\infty} \frac{e^{-ma}}{m^{p+1}} \, dm \quad \text{or,} \quad I(m) = \Gamma(p+1) \int_m^{\infty} \frac{e^{-ax}}{x^{p+1}} \, dx .$$

We have consequently:

$$I(1) = \Gamma(p+1) \int_1^{\infty} \frac{e^{-ax}}{x^{p+1}} \, dx$$

or,

$$\boxed{I_1 = \Gamma(p+1) \cdot e^a E_{p+1}(a)}$$

which is the result of the integration.

Consider next the integral

$$I_2 = \int_0^{\infty} \frac{z^p}{(z+a)^2} \, e^{-z} \, dz .$$

We note that

$$I_2 = - \frac{d}{da} \left\{ \int_0^{\infty} \frac{z^p}{(z+a)} \, e^{-z} \, dz \right\} = - \frac{dI_1}{da}$$

and we obtain by differentiation

$$I_2 = - \frac{d}{da} \left[\Gamma(p+1) \, e^a \, E_{p+1}(a) \right] = + \Gamma(p+1) \, e^a \left(E_p(a) - E_{p+1}(a) \right) .$$

The result is thus

$$\boxed{I_2 = \Gamma(p+1) \, e^a \left(E_p(a) - E_{p+1}(a) \right)}$$

We may expand this result further by considering

$$I_3 = \int_0^\infty \frac{z^p}{(z+a)^3} e^{-z} \, dz .$$

We write

$$I_3 = -\frac{1}{2} \frac{d}{da} \left\{ \int_0^\infty \frac{z^p}{(z+a)^2} e^{-z} \, dz \right\} = -\frac{1}{2} \frac{dI_2}{da}$$

or,

$$I_3 = -\frac{1}{2} \Gamma(p+1) \, e^a \left(- E_{p-1}(a) + E_p(a) + E_p(a) - E_{p+1}(a) \right)$$

or, finally:

$$\boxed{I_3 = \frac{1}{2} \Gamma(p+1) \, e^a \left(E_{p-1}(a) - 2E_p(a) + E_{p+1}(a) \right)}$$

The next step is

$$I_4 = \int_0^\infty \frac{z^p}{(z+a)^4} e^{-z} \, dz = -\frac{1}{3} \frac{d}{da} \left\{ \int_0^\infty \frac{z^p}{(z+a)^3} e^{-z} \, dz \right\} = \frac{1}{3} \frac{dI_3}{da}$$

giving

$$I_4 = -\frac{1}{3} \cdot \frac{1}{2} \Gamma(p+1) \, e^a \left(-E_{p-2}(a) + 2E_{p-1}(a) - E_p(a) + E_{p-1}(a) - 2E_p(a) + E_{p+1}(a) \right)$$

or,

$$\boxed{I_4 = \frac{1}{6} \Gamma(p+1) \, e^a \left(E_{p-2}(a) - 3E_{p-1}(a) + 3E_p(a) - E_{p+1}(a) \right)}$$

Although further generalisations are obvious, we shall not need them for our purposes.

EUROPEAN CENTRE FOR MEDIUM RANGE WEATHER FORECASTS

Directorate (D)
Technical Report No. 8

No. 1 A Case Study of a Ten Day Prediction

No. 2 The Effect of Arithmetic Precision on some Meteorological Integrations

No. 3 Mixed-Radix Fast Fourier Transforms without Reordering

No. 4 A Model for Medium-Range Weather Forecasting - Adiabatic Formulation -

No. 5 A Study of some Parameterizations of Sub-Grid Processes in a Baroclinic Wave in a Two-Dimensional Model

No. 6 The ECMWF Analysis and Data Assimilation Scheme - Analysis of Mass and Wind Fields

No. 7 A Ten Day High Resolution Non-Adiabatic Spectral Integration : A Comparative Study

Note : Technical Reports Nos 1 - 7 incl. were produced by the ECWMWF Research Department (RD)